4207

MEASUREMENT OF FIELD-SATURATED HYDRAULIC CONDUCTIVITY, SORPTIVITY AND THE CONDUCTIVITY-PRESSURE HEAD RELATIONSHIP USING THE "GUELPH PERMEAMETER"

W.D. Reynolds and D.E. Elrick
University of Guelph
Guelph, Canada

ABSTRACT

The "Guelph Permeameter" (GP) method provides simultaneous, in-situ measurements in the vadose zone of field-saturated hydraulic conductivity, K_{fs}, sorptivity, S, and the hydraulic conductivity (K) - pressure head (ϕ) relationship, $K(\phi)$.

The method involves measuring the steady-state rate of water recharge, Q (m^3s^{-1}), from a small cylindrical hole of radius, a (a = 0.02-0.05 m), in which a constant depth of water, H (m), is maintained. A simple "in-hole" Mariotte bottle device is used to establish and maintain H, and to measure the corresponding Q. Two or more (H,Q) data-pairs for each hole are substituted into four equations to obtain K_{fs}, S and the slope, α, of the (assumed) exponential $K(\phi)$ relationship.

Preliminary testing indicates that the time and volume of water required to complete a measurement depend on the initial wetness of the soil, the soil texture, and the H and a values. For H = 0.10-0.20 m and a = 0.02-0.03 m, measurements on sandy soils require on the order of 10-35 min. and 0.3-2.0 l of water. A loam soil at field capacity required 30-60 min. and 0.5-1.0 l of water, while a dry clay required on the order of 1.5-2.0 hours and 0.25-1.0 l of water.

Comparison of the GP method to the Air Entry Permeameter method on a loamy sand, a fine sandy loam, a silt loam and a clay produced within-soil type differences in mean K_{fs} of about a factor of 2. On a loam soil with macropore-induced vertical-horizontal anisotropy, K_{fs} values determined by the GP method effectively averaged the K values determined from vertically and horizontally oriented soil cores.

Attractive practical features of the GP method include speed, portability, low water use, simple equipment that is easily operated by one person, and, with the present apparatus, a practical measurement range of K_{fs} of about 10^{-4} - 10^{-8} ms^{-1} and the capability to depth profile to about 1 meter.

Enclosure 3
8.3.1.2.21

per-measurement basis are often still not feasible due to the extensive replication usually required to account for spatial variability (Carvallo et al., 1976; Nielsen et al., 1973).

This paper describes the recently developed Guelph Permeameter (GP) method (Reynolds and Elrick, 1986), which is capable of simultaneous, in-situ measurement of K_{fs}, S and α, and which is potentially simple and rapid enough to remain cost-effective even when extensive replication of measurements is required. Also included are two field comparisons of the GP method to established methods.

DESCRIPTION OF METHOD

The GP theory, apparatus, procedures for its use, and example calculations are given in detail in Reynolds et al. (1985) and Reynolds and Elrick (1986). The following is therefore only a summary of the essential elements and readers should refer to the above references.

1. Mode of Operation

The GP method measures the steady-state liquid recharge, Q (m^3s^{-1}), necessary to main a constant depth of liquid, H (m), in an uncased, cylindrical well of radius, a (m), finished above the water table. K_{fs}, S and α for infiltration (i.e. wetting) are then calculated from Q, H and a using the "Richards", "Laplace" and "Gardner" analyses (see below), which are based on steady-state solutions for infiltration into unsaturated soil from a well (Reynolds and Elrick, 1985; Reynolds et al., 1985).

2. Apparatus

The GP apparatus (Figure 1) is essentially an "in-hole" Mariotte bottle constructed of concentric, transparent plastic tubes. The inner "air-inlet tube" provides the air supply to the permeameter and the outer tubes provide the liquid reservoir (the "reservoir tube") and the liquid outlet (the "outlet tube") into the well. The air-inlet tube is inserted through the other tubes via a sliding, airtight (O-ring) seal in an airtight, removable cap on the top of the reservoir. The sliding seal allows convenient change of the H-level through adjustment of the height of the air-inlet tube. The removable cap provides the means for filling the reservoir tube with liquid. Liquid flows out of the outlet tube through a funnel-shaped "outlet port" located immediately above the permeameter tip. The permeameter tip is a perforated section of outlet tube filled with fine gravel. The gravel reduces the turbulence of liquid flow out of the permeameter during the initial filling to the H-level.

The permeameter operates by maintaining sufficient vacuum in the reservoir that liquid flows out through the tip at the rate required to keep the liquid level in the well (i.e. the H-level - see Figure 1) at the same height as the base of the air-inlet tube. With this system, the recharge from the well is obtained by simplying measuring the rate of fall of the liquid level in the permeameter. The

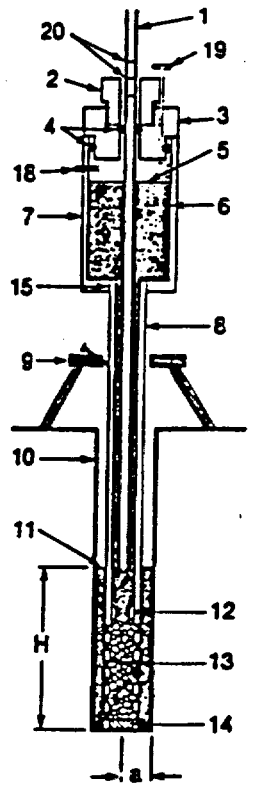

1. air-inlet tube (threaded at base)
2. threaded collar
3. removable cap
4. sliding air-tight seals
5. liquid surface in reservoir
6. measuring scale
7. reservoir tube
8. outlet tube
9. tripod assembly
10. well
11. steady liquid level in well
12. outlet port (threaded)
13. permeameter tip
14. rubber stopper
15. threaded coupling
18. pressure transducer (optional)
19. release valve
20. calibration lines

Figure 1: Schematic of the Guelph Permeameter (not to scale).

flow rate out of the permeameter (and therefore out of the well and into the soil) generally declines to a steady value (i.e. the Q value) within a short period of time.

The permeameter is presently designed for operation in uncased wells ranging in radius from 0.02 m to about 0.05 m and up to 1 m deep (approximate dimensions of the various components are given in Table 1). This was done primarily to allow the convenience and economy of digging the wells with a manual soil auger or probe. There are no theoretical restrictions (within limits) on the radius of either the well or the permeameter, however, and they can be altered to fit specific needs. The maximum depth at which measurements can be taken can be extended to the practical limit of Mariotte bottle operation, about 8 m, by simply increasing the length of the outlet and air-inlet tubes. For depths greater than 8 m, the GP theory and calculations still apply, but a different apparatus would be required to maintain H and to measure Q (such as the float valve-storage tank system commonly used in the shallow-well pump-in method - Bureau of Reclamation, 1978).

The present permeameter design has a practical measurement range of K_{fs} of about 10^{-4} ms^{-1} to $10^{-8}ms^{-1}$. (A smaller internal diameter (≈2cm) reservoir tube is often used for $K_{fs} = 10^{-7}$-$10^{-8}ms^{-1}$.)

Table 1. Approximate dimension of various components of the Guelph Permeameter.

		Inside Diameter	Wall Thickness	Length
		(cm)	(cm)	(cm)
Air-Inlet Tube		0.64	0.16	180-190
Reservoir Tube		5.72-10.80	0.32	40-70
Outlet Tube		2.70	0.32	100-140
Permeameter Tip:	Perforations		0.32 cm diameter	
	Length		2.0-6.0 cm	

3. Procedure

In essence, the procedure for taking a measurement consists of (refer to Figure 1 and Reynolds and Elrick, 1986):

(i) Excavating a cylindrical well to the desired depth in the material to be tested.
(ii) Filling the permeameter with liquid and inserting it in the well.
(iii) Starting the permeameter by raising the air-inlet tube out of the outlet port.
(iv) Setting the desired H-level by adjusting the height of the air-inlet tube.
(v) Monitoring the rate of fall, r, of the liquid surface in the reservoir until a steady rate, $\bar{r}$, is attained.
(vi) Calculating Q using $\bar{r}$ and the cross-sectional area of the reservoir.
(vii) Calculating K_{fs}, S and α using the provided equations (see Analysis section below).

Steps(iv)-(vii) must be repeated at least once if the Richards analysis (see below) is used, since it requires at least two (H,Q) data pairs.

4. Governing Equations

Steady-state discharge from a cylindrical well into unsaturated soil may be described by (Reynolds and Elrick, 1985),

$$2\pi H^2 K_{fs} + C\pi a^2 K_{fs} + 2\pi H \phi_m = CQ \quad , \qquad (2)$$

where ϕ_m ($m^2 s^{-1}$) is the matric flux potential, C is a dimensionless proportionality parameter and the rest of the variables are as previously defined. The first term on the left of Equation (2) represents the "hydraulic push" of liquid into the soil due to the hydrostatic pressure of the liquid in the well, the second term the "gravitational pull" of liquid out through the bottom of the well, and the third term represents the "matric pull" of liquid out of the well due to capillary forces in the surrounding soil. The first two terms

on the left of Equation (2) may be thought of as the "field-saturated" component of flow out of the well, and the third as the unsaturated flow component.

The matric flux potential, ϕ_m, is defined as (Gardner, 1958),

$$\phi_m = \int_{\psi_i}^{\bullet} K(\psi)d\psi \; ; \; -\infty < \psi_i < 0 \; , \qquad (3)$$

where $K(\psi)$ is the hydraulic conductivity-pressure head relationship for infiltration and ψ_i is assumed uniform in the vicinity of the well. Assuming the "Green and Ampt" soil of Philip (1969), it can be shown that (Philip, 1973),

$$S = \sqrt{2\,(\Delta\theta)\phi_m} \; , \qquad (4)$$

where $\Delta\theta$ is the change in liquid content in the soil adjacent to the well from the initial value (ϕ_i) to the field-saturated value (θ_{fs}). In addition, substituting Equation (1) into (3) and integrating produces ,

$$\phi_m = \frac{K_{fs}}{\alpha}[1 - \exp(\alpha\psi_i)], \qquad (5)$$

which for many soils at "field capacity" or drier effectively simplifies to (Scotter et al., 1982),

$$\alpha = K_{fs}/\phi_m \; . \qquad (6)$$

Combining α with K_{fs} in Equation (1) determines the "integrally correct" exponential $K(\psi)$ relationship of the porous medium. Parlange et al. (1985) shows that this α value (referred to as an "absorptive length" in Philip, 1985) is dependent on both porous medium properties and ψ_i.

Numerical simulations of steady saturated-unsaturated flow around the well indicate that the C parameter in Equation (2) is primarily a function of the H/a ratio with a secondary dependence on soil type. (There are also additional minor dependencies on proximity of the liquid surface in the well to the soil surface, ψ_i, and the magnitudes of H and a .). In Figure 2, C versus H/a relationships are given for a coarse sand ($K_{fs} = 10^{-4}$ ms^{-1}, $\alpha = 25$ m^{-1}), Guelph loam ($K_{fs} = 3.7 \times 10^{-6}$ ms^{-1}, $\alpha = 3.4$ m^{-1}) and unstructured heavy clay ($K_{fs} = 10^{-8}$ ms^{-1}, $\alpha = 0.1$ m^{-1}), which covers the range of most practical applications. Most loams and structured clays should be adequately represented by the Guelph loam curve. Strictly speaking, there curves apply only for soils at field capacity and drier and when the wetting front from the well does not appear on the soil surface.

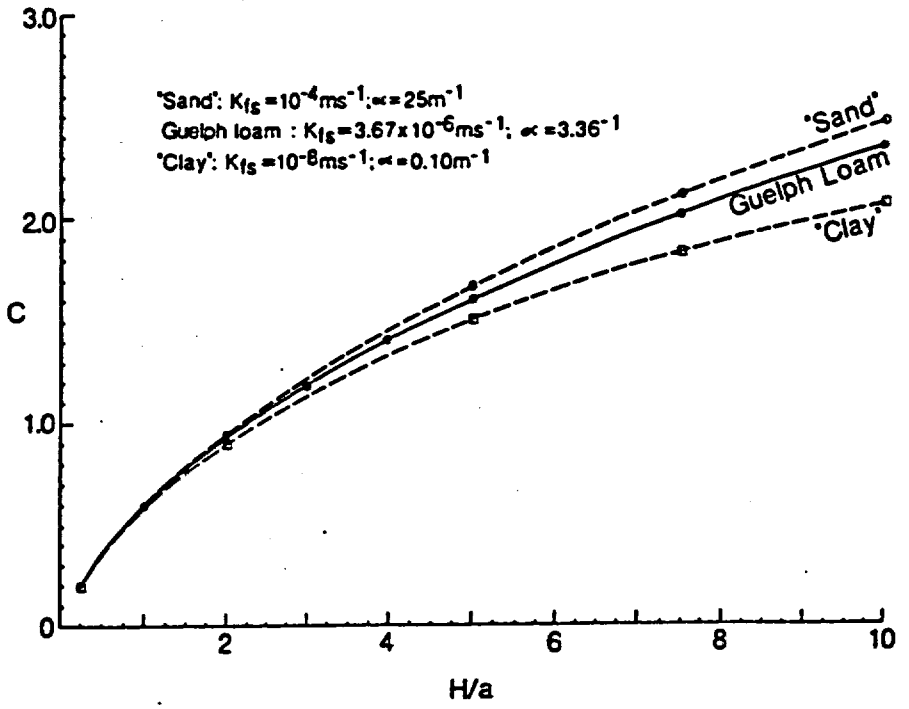

Figure 2: C versus H/a relationship for a range of soil textures. Curves apply for soils at field capacity and drier. Most loams and structured clays should be adequately represented by the Guelph loam curve.

ANALYSES

1. Richards Analysis

The Richards analysis uses 2 or more successively ponded H-levels in one well (i.e. H_1, H_2, etc.) and their corresponding Q values (i.e. Q_1, Q_2, etc.) (see Reynolds and Elrick, 1986 for detailed procedure). K_{fs} and ϕ_m are obtained from,

$$K_{fs} = \frac{\sum_{i=1}^{n} H_i^2 \sum_{i=1}^{n} C_i Q_i \left(\frac{C_i a_i^2}{2} + H_i^2\right) - \sum_{i=1}^{n} H_i C_i Q_i \sum_{i=1}^{n} H_i \left(\frac{C_i a_i^2}{2} + H_i^2\right)}{2\pi \left\{ \sum_{i=1}^{n} H_i^2 \sum_{i=1}^{n} \left(\frac{C_i a_i^2}{2} + H_i^2\right)^2 - \left[\sum_{i=1}^{n} H_i \left(\frac{C_i a_i^2}{2} + H_i^2\right)\right]^2 \right\}} \quad (7)$$

$$\phi_m = \frac{\sum_{i=1}^{n} C_i Q_i \left(\frac{C_i a_i^2}{2} + H_i^2\right) \sum_{i=1}^{n} H_i \left(\frac{C_i a_i^2}{2} + H_i^2\right) - \sum_{i=1}^{n} H_i C_i Q_i \sum_{i=1}^{n} \left(\frac{C_i a_i^2}{2} + H_i^2\right)^2}{2\pi \left\{ \left[\sum_{i=1}^{n} H_i \left(\frac{C_i a_i^2}{2} + H_i^2\right)\right]^2 - \sum_{i=1}^{n} H_i^2 \sum_{i=1}^{n} \left(\frac{C_i a_i^2}{2} + H_i^2\right)^2 \right\}} \quad (8)$$

where n is the number of H-levels used (n≥2), and C_i and Q_i are the C and Q values corresponding to the chosen H-levels (i.e. H_i) and well radius (a). It should be noted that Equations (7) and (8) can also handle multiple well radii (a_i); however, it has been found that the analysis works best when a single well is used (i.e. $a_i = a =$ constant).

2. Laplace and Gardner Analyses

If only "ball park" K_{fs} or ϕ_m values are required, simpler and less labour-intensive approximations, the Laplace and Gardner analyses, can sometimes be applied. Both of these analyses require only one H-level.

The Laplace analysis has the form,

$$K_{fs}^1 = \frac{CQ}{(2\pi H^2 + C\pi a^2)} , \qquad (9)$$

and the Gardner analysis is,

$$\phi_m^1 = \frac{CQ}{2\pi H} . \qquad (10)$$

The Laplace and Gardner analyses ignore capillarity and field-saturated flow, respectively (ref. Equation 2), with the result that $0 < K_{fs} < K_{fs}^1$ and $0 < \phi_m < \phi_m^1$ (Reynolds and Elrick, 1985). The overestimate of K_{fs} by K_{fs}^1 decreases as the ϕ_m of the soil decreases (i.e. as α and/or ϕ_i increase; which effectively translates to coarse and/or wet porous media), and K_{fs}^1 equals K_{fs} at field-saturation when $\phi_m = 0$. Similarly, the overestimate of ϕ_m by ϕ_m^1 decreases as K_{fs} and/or ϕ_i decreases (i.e. fine and/or dry porous media). Preliminary field investigations (see below) suggest that K_{fs}^1 and ϕ_m^1 are often sufficiently accurate for many practical applications when the appropriate soil textures and moisture conditions prevail.

PERFORMANCE

1. Time and Volume of Liquid Required per Measurement

The time and volume of liquid required to complete a measurement depend on the initial wetness of the porous medium, the porous medium texture, and the H and a values. Generally speaking, the drier and the finer the texture of the porous medium, the larger the H and a values, and the larger the H/a ratio, the greater the time and/or liquid requirement per measurement. For H = 0.10-0.20 m and a = 0.02-0.03 m, measurements on some sandy soils at moisture contents close to field capacity required on the order of 10-20 minutes and 0.3-1.0 liters of water (Lee et al., 1985). Dry sand soils on the other hand, often require on the order of 15-35 minutes and up to 2 liters of water (D.E. Elrick, unpublished data). A loam soil close to capacity was found to require 30-60 minutes and 0.5-1.0 liters of water (W.D. Reynolds, unpublished data), while a dry clay required on the order of 1.5-2.0 hours and 0.25-1.0 liters of water (Lee et al., 1985). These ranges should be used only as general indicators, however, since field testing is still limited.

2. Assessment of Results

Heterogeneity in the porous medium can result in unrealistic calculations of K_{fs}, ϕ_m, S and α when using the Richards analysis. When a significant heterogeneity, such as a large macropore or a layer boundary, is encountered between two H-levels, the calculations based on those H-levels may yield a negative K_{fs} or ϕ_m value. Both values (i.e. the positive one as well as the unrealistic negative one) should be discarded when this ocurs (Reynolds and Elrick, 1985). A persistent problem of negative values can often be minimized by successively ponding 3 or more H-levels. This approach tends to average out the variation between the H-levels, producing a weighted mean K_{fs} and ϕ_m. A further check is provided by the Laplace and Gardner analyses. Since K_{fs}^1 and ϕ_m^1 overestimate K_{fs} and ϕ_m, respectively, K_{fs} and ϕ_m values that are significantly greater than the corresponding K_{fs}^1 and ϕ_m^1 estimates should be treated with caution. Reynolds and Elrick (1985) conclude that a K_{fs} - ϕ_m measurement by the Richards analysis is accurate when both are positive, and both are lower than their corresponding K_{fs}^1 and ϕ_m^1 estimates. One can also avoid negative values completely by replacing K_{fs} or ϕ_m with K_{fs}^1 or ϕ_m^1, which, as mentioned above, does not introduce important error when the right soil and moisture conditions exist.

3. Sensitivity to C-Value

As shown in Figure 2, the C versus H/a relationship is mildly dependent on porous medium texture and macroporous structure. Since texture and/or structure might not always be accurately known, it is important to have a feeling for how sensitive the K and ϕ_m analyses are to the choice of C.

The Laplace and Gardner analyses (Equations 9 and 10, respectively) clearly have a low sensitivity to C because C appears in them as linear terms. Consequently, the maximum change in the K_{fs}^1 and ϕ_m^1 estimates that can be induced is approximately equal to the discrepancy between the sand and unstructured clay C-values, which in Figure 2 increases to only 20% at H/a = 10.

The C-value is highly non-linear in the Richards analyses (Equations 7 and 8) and therefore sensitivity cannot be assessed in a straightforward manner. It was decided that the best indication would be obtained using actual field data. Q, H and a data from the second field comparison discussed below (see Section 4, (ii)) were combined with the appropriate sand, loam and clay C-values, and K_{fs}, ϕ_m, S and α calculated. The results are given in Table 2. It is seen that for each well radius the maximum change in $\overline{K}_{fs}$ and $\overline{S}$ is only 30-40%, which is of little consequence for most practical applications. The $\overline{\phi}_m$ and $\overline{\alpha}$ values, on the other hand, are more sensitive, changing by a factor of about 2-3. This is at least partially due to the wet state of the soil (approximately field capacity) during the measurements and the resulting small ϕ_m values (i.e. as $\psi_i \to 0$, $\phi_m \to 0$ and ϕ_m consequently becomes more sensitive to errors and perturbations).

Table 2: Sensitivity of K_{fs}, ϕ_m, S and α calculations to the choice of C-value. Actual field data used.

		Well Radius (a)*	
		0.02m	0.03m
$10^6 K_{fs}$ + (ms^{-1})	Sand C's ‡	1.27	2.57
	Loam C's	1.20	2.20
	Clay C's	0.968	2.04
$10^7 \bar{\phi}_m$ + ($m^2 s^{-1}$)	Sand C's ‡	0.294	0.778
	Loam C's	0.349	1.33
	Clay C's	0.560	1.36
$10^4 \bar{S}$ + ($ms^{-1/2}$)	Sand C's ‡	0.940	1.53
	Loam C's	1.02	2.00
	Clay C's	1.30	2.02
$\bar{\alpha}$ + (m^{-1})	Sand C's ‡	43.1	33.1
	Loam C's	34.2	16.5
	Clay C's	16.7	14.9

* - H-levels of 0.10 m and 0.15 m were used to yield H/a ratios of 3.3, 5.0 and 7.5

\+ - Geometric mean values - Richards analysis used

‡ - The "Loam C's" are the correct values for the soil tested (see Section 4, (ii)).

4. Field Comparisons

(i) Comparison of the GP method (using the Laplace analysis) to the Air Entry Permeameter method and a soil core method on a range of soil types.

The GP method was compared to the Air Entry Permeameter (AEP) method (Topp and Binns, 1976) and the falling head soil core (SC) method (see Lee, 1984) on a loamy sand, a fine sandy loam, a silt loam and a clay at four separate 100 m^2 area sites. The AEP method is in-situ (like the GP method), while the SC method is a laboratory determination on an "undisturbed", vertically oriented soil core taken from the field. Average soil physical characteristics for the 4 sites are given in Table 3. Twenty K measurements (with 2 exceptions - see Table 4) were taken at each site with each method. The measurements were taken at aproximately 1.5 m intervals in a square grid pattern and the 3 methods were alternated throughout the grid. All sites were below field capacity when tested. Further details on procedure and experimental design can be found in Lee (1984) and Lee et al. (1985).

Table 3: Field comparison (i) : Soil physical characteristics averaged over 0-0.30 m depth.

Soil Series	Sand (%)	Silt (%)	Clay (%)	O.M. (%)
Fox loamy sand	86	9	5	0.5
Vineland vfs loam	64	24	12	2.3
Woolwich sl loam	28	52	20	2.3
Trafalgar clay	5	33	63	4.2

The AEP method, like the GP method, measures a field-saturated hydraulic conductivity (K_{fs}), while the SC method can measure a truly saturated conductivity (K_s). Work by Bouwer (1966) and Stephens et al. (1983, 1984) indicates, however, that reasonably accurate estimates of K_s can usually be obtained from the AEP and GP methods by simply multiplying the K_{fs} measurement by 2. The AEP and GP methods can therefore be compared on both a K_{fs} and a K_s basis, and all three methods can be compared on a K_s basis. The Laplace analysis was used to calculate K_{fs} in the GP method (i.e. K_{fs} was calculated using Equation 9).

The geometric mean K_{fs} and K_s values ($\overline{K}_{fs}$ and $\overline{K}_s$, respectively) for the three methods at the 4 sites are given in Table 4. (The geometric mean was used because K was found to be log-normally distributed - Warrick and Nielsen, 1980). Also included in Table 4 are the ranges (R) and coefficients of variation (CV) of the measurements, as well as the failure rates (FR) and the average estimated time to obtain a K measurement (T). The FR was calculated by dividing the number of failed attempts to obtain a K measurement by the total number of attempts and multiplying by 100. A "failed attempt" was any attempt that did not produce a K value. The T value includes the time to prepare and install the apparatus as well as the time spent taking readings. Only successful K measurements are included in the T value.

It is seen in Table 4 that the $\overline{K}_{fs}$ and $\overline{K}_s$ values for the AEP and GP methods are significantly different (at the 1% level) only for the sand soil, where the GP method yields a higher value. This higher value is not surprising since the Laplace analysis, which overestimates K_{fs}, was used. Although not statistically significant, the $\overline{K}_{fs}$ and $\overline{K}_s$ values in the loam and clay soils exhibit the reverse trend, the AEP method yielding values about a factor of 2 higher than the GP method. This is considered to represent combined effects of sample size, flow geometry and response to macropores (i.e. cracks, worm holes, root channels, etc.). The AEP method verticially infiltrates water under a

Table 4: Field comparison (i): Geometric means ($\overline{K}_{fs}$ and $\overline{K}_s$), range (R) and coefficient of variation (CV) from the 20 measurements by each method on the 4 soils. The failure rate (FR) in obtaining the 20 measurements and the estimated time to obtain a K measurement (T) are also given.

Soil Series	Method	$10^6\overline{K}_{fs}$ (ms^{-1})	$10^6\overline{K}_s$ (ms^{-1})	R (Orders of Magnitude)	CV (%)	FR (%)	T‡ (min)
Fox loamy sand	AEP[1]	16.9a+	33.7a+	0.9	52	0	20
	GP[2]	28.8b	57.6b	1.1	75	10	10-15
	SC[3]	-	20.6c	1.0	69	5	125
Vineland vfs loam	AEP	2.03a	4.06a	1.5	147	15	50-55
	GP	0.945a	1.89ab	1.1	81	0	50
	SC	-	0.74b	2.2	260	10	1500
Woolwich sl loam	AEP	1.35a	2.70a	1.6	128	25	80-95
	GP	0.930a	1.86a	0.7	57	5	80
	SC	-	0.62b	1.2	111	0	1500
Trafalgar clay	AEP*	0.101a	0.202a	2.6	519	64	160-170
	GP	0.053a	0.106ab	2.9	635	30	90-100
	SC*	-	0.025b	2.7	562	25	2000-3000

AEP[1] - Air Entry Permeameter
GP[2] - Guelph Permeameter
SC[3] - Soil Cores
* - n = 18, n = 20 otherwise
\+ - within each soil type, a different alphabetic character indicates a significantly different $\overline{K}$ at the 1% level according to a two-tailed, pair-wise t-test (Snedecor, 1957, pp.85-101).
‡ - includes time required for apparatus installation and preparation as well as measurement time.

high positive head (about 1 m) across a horizontal, 500 cm^2 surface area. The GP method, on the other hand, infiltrates water radially across a vertical, 250 cm^2 surface area at a pressure head varying linearly from zero at the water surface in the well to H at the base of the well (in this study H=0.20 m and a=0.02 m). Since macropores have a preferential vertical orientation, it can be expected that the AEP method will tend to intersect more macropores per measurement than the GP method. Also, due to the higher applied pressure head, these macropores should have a proportionately greater influence on the AEP measurement than on the GP measurement.

The consistently lower $\overline{K}_s$ values yielded by the SC method is considered to be a combined sample size-procedure effect. Very small 0.05 m diameter by 0.03 m long cores were used. It is therefore possible that proportionately fewer macropores are included per measurement than with the other methods (i.e. sampling was biased

toward the soil matrix). Also, soil cores with large, continuous macropores vented at both top and bottom sometimes failed to produce K_s measurements because the rate of fall of the water level in the stand-pipe (the falling head procedure was used) was too fast to measure. Consequently, the "high end" of the data set may have been lost.

The FR values given in Table 4 reveal a disturbing feature of the K estimates. The $\overline{K}$ values reflect the contribution of only those values of K for which the method was successful. The failures may be the result of some natural physical property of the soil affecting K, such as stones, layering, macropores, slaking, swelling, etc., which is not adequately accounted for by the measurement technique. If this is actually the case, the $\overline{K}$ estimate obtained when a high FR occurs is probably not as representative of the true value as one would like. It is seen from Table 4 that each method achieves a 0 FR for only one particular soil type, and that all three methods have high FR values for the clay soil. This may indicate that if maximum accuracy in $\overline{K}$ is required, usage of the methods should be restricted to certain soil types or range in soil types, and that all three methods are suspect in clay soils. In this study, the AEP method has the highest total FR while the GP and SC methods are about the same, regardless of whether the clay soil is included or excluded.

For most practical applications the discrepancy between the AEP and GP results (about a factor or 2) is probably not important. However, the generally lower FR and T values and the significantly lower equipment, personnel and operator skill requirements of the GP method (discussed in Lee, 1984; Lee et al., 1985; Reynolds and Elrick, 1986) are considered to give it a distinct advantage.

(ii) Comparison of the GP and SC methods on a heterogeneous, anisotropic loam soil

The GP method was compared to a constant head soil core (SC) method (Elrick et al., 1981) on a $15m^2$ area of heterogeneous, anisotropic "Guelph loam" soil. Soil physical characteristics and cropping history are given in Table 5. Fourteen paired, vertically and horizontally oriented, "undisturbed", 0.05 m diameter by 0.05 m long soil cores were taken at random over the site (i.e. a total of 28 cores were taken). The GP method used eleven 0.02 m radius wells and eleven 0.03 m radius wells (for a total of 22 wells) which were also randomly located over the site. Within each well, 2 H-levels, H_1 = 0.10 m and H_2 = 0.15 m, were successively ponded (with no interrum drainage allowed) to obtain Q_1 and Q_2, respectively. The measurements were taken at the end of the growing season (October) with a crop of field corn still in place. The wells and cores were located on the site as indicated in Figure 3. Further detail on procedures and experimental design can be found in Reynolds and Elrick (1985).

Plots of cumulative probability versus lnK for the GP and SC results are given in Figures 4, 5 and 6. In Figure 4 the GP K-values are calculated using the Laplace analysis (K_{fs} - Equation 9), in Figure

Table 5: Field comparison (ii) : Soil physical characteristics.

Soil Series:	Guelph Loam
Horizonation:	Ap(k) 0-0.25m (2%-10% stones by volume) Bt 0.21m-0.28m (discontinuous) Ck >0.25m (>15% stones by volume)
Primary Stratigraphy*:	None evident
Macroporous Structure:	- Primarily vertically oriented worm holes and root channels - Some planar voids in Bt
Slope:	8%
Cropping History:	- Continuous corn for approximately 20 years - Stover removed

Textural Analysis:

Depth (m)	Sand (%)	Silt (%)	Clay (%)	O.M. (%)
0.00-0.05	42	42	16	3.1
0.05-0.10	41	43	17	3.1
0.10-0.15	40	43	17	2.7
0.15-0.20	40	43	17	2.6
0.20-0.25	42	44	15	1.8
0-25-0.30	47	40	14	0.8
0.30-0.35	48	39	13	0.7
0.35-0.40	49	40	12	0.6
0.40-0.45	50	41	11	0.5
0.45-0.50	51	41	9	0.3

* "Primary Stratigraphy" means visually detectable textural layers produced by sedimentary processes.

5 they are calculated using the Richards analysis (K_{fs} - Equation 7), and in Figure 6 the Richards K_{fs} values are converted to K_s values (i.e. $K_s = 2K_{fs}$). Since the Laplace analysis requires only one H-level and its corresponding Q value, there are 2 K_{fs}^1-values per well in Figure 4 for a total of 44 K_{fs}^1 values. The Richards analysis, on the other hand, requires at least 2 H-levels to obtain K_{fs}, and thus there is only one K_{fs} value per well in Figures 5 and 6. Fewer than 22

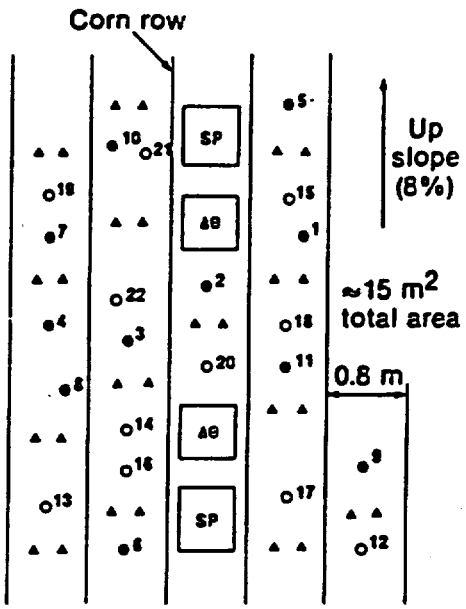

Figure 3: Field comparison (ii) : Sample locations

K_{fs}-values appear in Figures 5 and 6 because heterogeneities caused some of the K_{fs} and ϕ_m values to be negative. It should also be mentioned that since the data in Figures 4, 5 and 6 form approximate straight lines, log-normal distributions were assumed (as with field comparison (i)) in all statistical analyses (Warrick and Nielsen, 1980).

The SC values in Figures 4, 5 and 6 are seen to effectively bracket the GP values, the vertically oriented cores forming the "high K" boundary and the horizontal cores the "low K" boundary. The slopes of the SC and Richards distributions (Figures 5 and 6) are very similar, while the slopes of the Laplace distributions (Figure 4), although similar to each other, are somewhat steeper. The K_{fs} values in Figure 5 appear to be weighted toward the horizontal core values; however, when they are corrected for entrapped air in Figure 6 (i.e. converted to K_s values) they plot approximately midway between the two core distributions. Overall, the GP means appear to be averaging the vertical and horizontal K_s on this site.

A statistical comparison of the SC and GP results given in Table 6 confirms the indications of Figures 4, 5 and 6. The vertically oriented cores yield a significantly higher $\overline{K}_s$ than the horizontally oriented cores, while the GP means lie inbetween.

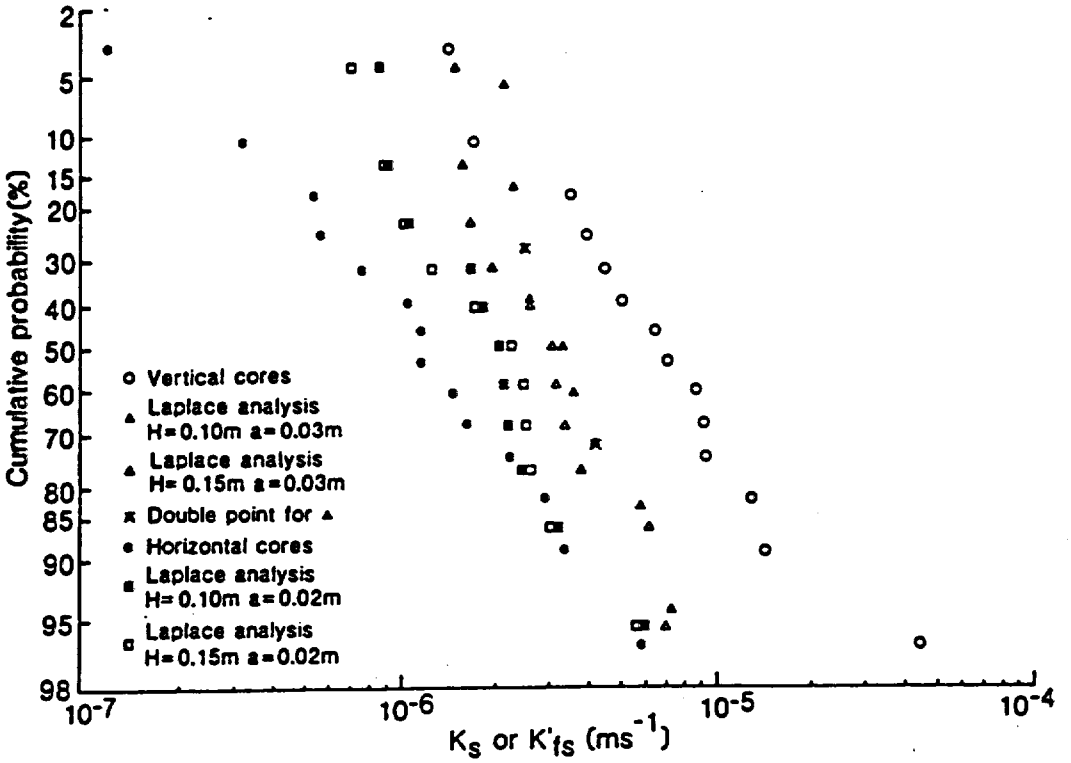

Figure 4. Field comparison (ii): Cumulative probability versus lnK for soil cores (K_s) and the Laplace analysis (K'_{fs}).

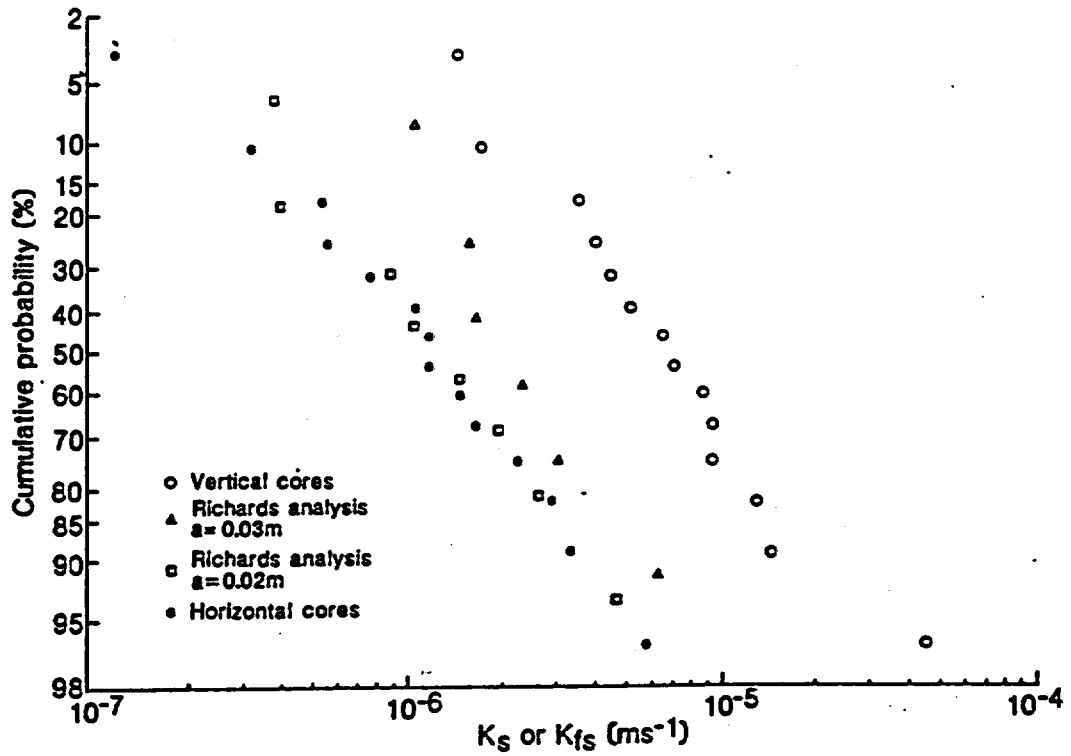

Figure 5. Field comparison (ii): Cumulative probability versus lnK for soil cores (K_s) and the Richards analysis (K_{fs}).

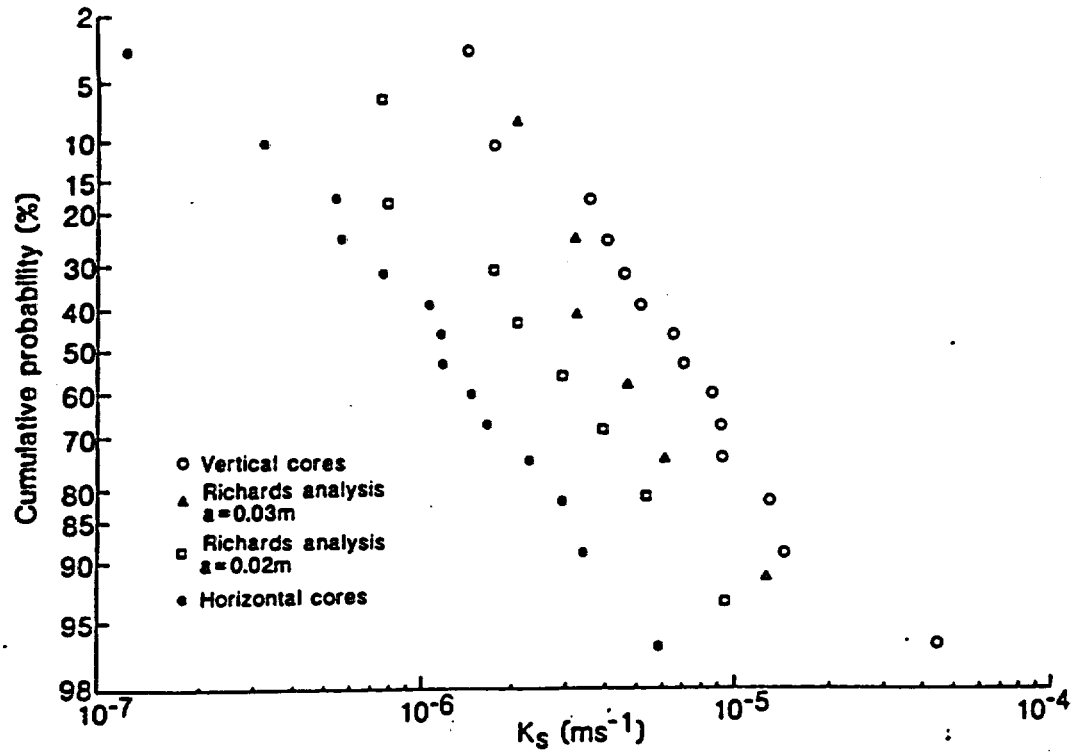

Figure 6. Field comparison (ii): Cumulative probability versus lnK for soil cores (K_s) and the Richards analysis K_{fs} values converted to K_s values ($K_s = 2K_{fs}$).

The matric flux potential (ϕ_m), sorptivity (S) and α-parameter results for field comparison (ii) are given in Table 7. Although no independent data are available for direct comparison, the literature indicates that the $\overline{S}$ and $\overline{\alpha}$ values are plausible for this soil type and conditon.

It is noted in Tables 6 and 7 that the $\overline{K}$, $\overline{\phi}_m$, and $\overline{S}$ values for the 0.03 m radius wells are higher than their coresponding values for the 0.02m radius wells, while the $\overline{\alpha}$, Range and CV values exhibit the reverse trend. This is considered to represent a sample size effect, particularly since the two well radii form separate distributions in Figures 4, 5 and 6. The 0.03 m radius wells sample a larger volume of soil. The larger volume averages over more heterogeneities and it has been shown that this often results in a lower CV and a higher $\overline{K}$ (Talsma, 1965; Willardson and Hurst, 1965; Starr et al., 1984). Considering the nature of the macroporous structure (i.e. primarily vertically oriented worm holes and root channels - see Table 4) and the SC results, it is also plausible that the greater total surface area of the 0.03 m radius wells encounters sufficiently more macropores to account for the higher $\overline{K}$, $\overline{\phi}_m$ and $\overline{S}$ values.

Table 6: Field comparison (ii) : Comparison of GP and SC results

Parameter	Vertical Cores	Laplace* H=0.10m a=0.03m	Laplace H=0.15m a=0.03m	Richards+ a=0.03m	Laplace H=0.10m a=0.02m	Laplace H=0.15 a=0.02m	Richards a=0.02m	Horizontal Cores
$10^6 K_{fs}$ ‡ (ms^{-1})		3.36	2.84	2.20	1.89	1.85	1.20	
$10^6 K_f$ ‡ (ms^{-1})	6.39	6.72	5.68	4.40	3.78	3.70	2.40	1.08
CV (%)	109	41	56	69	62	67	109	135
Range (Orders of Magnitude)	1.50	0.527	0.666	0.781	0.847	0.901	1.10	1.72
No. of Measurements	14	11	11	6	11	11	8	14
$ Statistical Comparison of Means (1%)	$\bar{K}_{fs}$ **							
	$\bar{K}_s$ ++							

* - GP - Laplace analysis (Equation 9)
\+ - GP - Richards analysis (Equation 7)
‡ - Geometric mean values
$ - Methods underscored by the same line do not have a significantly different $\bar{K}$ at the 1% level according to a pairwise Tukey (hsd) test (Steel and Torrie, 1980, p.192).
** -Comparison of $\bar{K}_{fs}$ values from the GP method to the $\bar{K}_s$ values from the SC method.

Table 7: Field comparison (ii) : Matric flux potential (ϕ_m), sorptivity (S) and α-parameter values. The S and α values were obtained using Equations (4) and (6) and the Richards estimates of ϕ_m.

Parameter	Gardner* H=0.15m a=0.03m	Gardner H=0.10m a=0.03m	Richards+ a=0.03m	Gardner H=0.15m a=0.02m	Gardner H=0.10m a=0.02m	Richards a=0.02m
$10^7\overline{\phi_m}^b$ (m^2s^{-1})	4.40	3.56	1.33	2.82	1.96	0.349
CV[c] (%)	56	41	61	67	62	232
Range[c] (Orders of Magnitude)	0.666	0.527	0.650	0.901	0.847	1.60
$10^4\overline{S}^{bd}$ ($ms^{-1/2}$)			2.00			1.02
$\overline{\alpha}^b$ (m^{-1})			17			34

* - GP - Gardner analysis (Equation 10)
\+ - GP - Richards analysis (Equation 8)
b - Geometric mean values
c - Applies only to the ϕ_m values
d - $\Delta\theta$ = 0.15

The differences between the Richards and Laplace $\bar{K}$ values in this study are small enough, a factor of about 1.6 for both well radii, to be unimportant for many practical applications. The Richards and Gardner $\bar{\phi}_m$ values, on the other hand, differ by significant amounts - by a factor of about 3 for the 0.03 m radius wells, and by a factor of about 6-8 for the 0.02 m radius wells. This is considered to be due primarily to the fact that the soil was near field capacity during the measurements. As indicated above, for a given porous medum the Laplace analysis becomes more accurate with increasing wetness while the Gardner analysis becomes less accurate.

Perhaps the most important indication of this field comparison is that the GP method appears to average vertical and horizontal anisotropy in K. This capability should be particularly useful in the design and monitoring of drainage and waste disposal systems that rely on three-dimensional saturated-unsaturated flow.

ADVANTAGES AND DISADVANTAGES OF THE GP METHOD

Some of the primary disadvantages and advantages of the GP method are as follows:

1. <u>Disadvantages</u>

   (i) Digging implements tend to smear the walls of the well in moist-to-wet porous media containing a significant amount of clay. (A smear layer generally appears as a smooth or "polished" surface.) There is also a tendency for "silting up" of the wall in porous media high in silt and clay. Since all the water must flow through the wall and base of the well, any partial sealing of these surfaces by smearing or siltation generally results in an unrepresentatively low Q value (and correspondingly unrepresentative K_{fs}, ϕ_m, S and α values). Providing that the well surfaces are not very wet, they can usually be adequately de-smeared with a small spiked wheel mounted on a handle (see Figure 7). When the wheel is run up and down the well wall several times the smear layer is broken up and plucked off by the sharpened, paddle-shaped spikes. Siltation of the well is due primarily to dislodgement of silt and clay from the well wall during the intial filling, and its subsequent "plating out" back onto the wall during the course of the measurement. This can usually be minimized by slow initial filling of the well, and/or by back-filling around the permeameter with coarse sand or fine gravel. In porous media that are particularly susceptible to siltation addition of flocculent to the permeameter liquid may also be advisable (providing that it does not change the permeability characteristics of the medium).

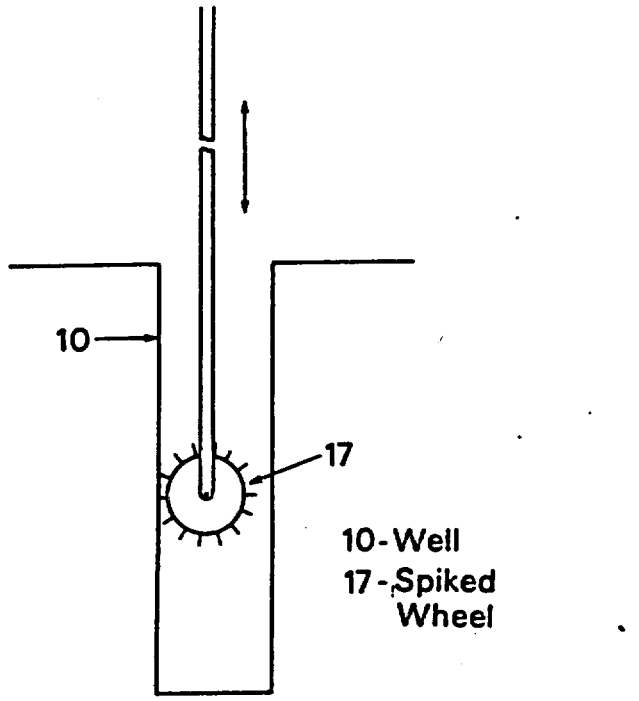

Figure 7: Apparatus for smear layer removal.

(ii) In extremely heterogeneous porous media a high percentage of the Richards analysis results can yield unrealistic (i.e. negative) K_{fs} and ϕ_m estimates. At present, the only procedures for dealing with this problem are to increase the replication until an adequate number of valid measurements are obtained, or to switch to the Laplace (or Gardner) analysis.

(iii) The α calculation assumes that the $K(\phi)$ relationship of the porous medium can be adequately described by Equation (1). This assumption will probably have varying degrees of validity for different porous media.

(iv) The method yields essentially a "point" measurement and therefore usually requires replication.

2. Advantages

(i) The method should yield simultaneous, in-situ measurements of K_{fs}, S and $K(\phi)$ (via the α estimate and Equation 1) for

infiltration of essentially any wetting liquid that can be put into the apparatus. It is therefore (potentially) possible to directly measure three of the most important physical parameters governing the infiltration and movement of contaminants and leachates, in addition to those governing infiltration and movement of water.

(ii) The method can be used to obtain vertical profiles of K_{fs}, S and α. After a measurement is completed at a given depth, the well is simply advanced to a greater depth (past the wetted zone) and a new measurement taken. This should make the GP method useful for in-situ determinations of three-dimensional K_{fs}, S and $K(\phi)$ distributions.

(iii) The GP apparatus is inexpensive, simple and easily operated by one person. In fact, in low permeability materials it is often possible for one operator to run several permeameters simultaneously. Also, the GP apparatus is sufficiently portable and durable, and has a sufficiently low liquid use per measurement, that in areas of limited accessibility one person can carry 2 or 3 permeameters, the support equipment, and enough liquid to operate for several hours.

(iv) The method usually requires less time per measurement than other methods and does not require extensive operator skill or training.

(v) Since the method uses little equipment and causes only slight disturbance to the porous medium, it can often be used on surfaces that do not have a high tolerance to disturbance or to large/heavy equipment (such as between the rows of crops, on sod farms, golf courses and lawns, on the caps and liners of landfills, reservoirs, canals, etc.).

(vi) The method has a theoretical foundation (as opposed to an empircal one) and measures physically well-defined parameters (i.e. K_{fs}, ϕ_m, S).

CONCLUDING REMARKS

The Guelph Permeameter method provides a cost-effective means for simultaneous, in-situ measurement of K_{fs}, S and $K(\phi)$, which are three of the main parameters governing flow of water and other wetting liquids in the vadose zone.

The method is well-founded theoretically and takes the major elements of saturated-unsaturated flow into account.

The apparatus is simple, durable, portable, inexpensive and easily operated by one person.

Data anlaysis is straightforward and yields physically based parameters. Options in the analysis procedure allow the accuracy of

the data to be assessed (i.e. cross-comparison of Richards, Laplace and Gardner analyses).

The method produces results quickly (within a few minutes to a couple of hours) and requires only small volumes of liquid per measurement.

Field comparisons to other methods, although still limited, confirm the method's validity.

The Guelph Permeameter apparatus is commercially available from Soilmoisture Equipment Corporation, Santa Barbara, California.

REFERENCES

Boersma, L. 1965. Field measurment of hydraulic conductivity above a water table. In: Methods of Soil Analysis, Pt. 1. C.A. Black (ed). Agronomy no. 9, pp.234-252. American Society of Agronomy. Madison, Wis.

Bouwer, H. 1966. Rapid field measurement of air entry value and hydraulic conductivity of soil as significant parameters in flow system analysis. Water Resources Research, v.2, no.4, pp. 729-738.

Bouwer, H. 1978. Groundwater Hydrology. McGraw-Hill. Toronto, Ont. 480 pp.

Bouwer, H. and R.D. Jackson. 1974. Determining soil properties. In: Drainage for Agriculture. J. van Schilfgaarde (ed.).. Agronomy, no.17, pp.611-672. American Society of Agronomy. Madison, Wis.

Bresler, E. 1978. Analysis of trickle irrigation with application to design problems. Irrigation Science, v.1, no.1, pp.3-17.

Bureau of Reclamation. 1978. Drainage Manual. U.S. Department of the Interior. Superintendent of Documents, U.S. Gov. Printing Office, Washington, D.C., pp.74-97.

Carvallo, H.O., D.K. Cassel, J. Hammond and A. Bauer. 1976. Spatial variability of in-situ unsaturated hydraulic conductivity of Maddock sandy loam. Soil Science, v.121, no.1, pp.1-8.

Clothier, B.E. and D.R. Scotter. 1982. Constant-flux infiltration from a hemispherical cavity. Soil Science Society of America Journal, v.46, no.4, pp.696-700.

Elrick, D.E., R.W. Sheard and N. Baumgartner. 1981. A simple procedure for determining the hydraulic conductivity and water retention of putting green soil mixtures. Proc. IV Int. Turfgrass Res. Conf., Guelph, pp.189-200.

Gardner, W.R. 1958. Some steady-state solutions of the unsaturated moisture flow equation with application to evaporation from a water table. Soil Science, v.85, no.4, pp.228-232.

Hillel, D. 1980a. Fundamentals of Soil Physics. Academic Press. Toronto, Ont. 413 pp.

Hillel, D. 1980b. Applications of Soil Physics. Academic Press. Toronto, Ont. 385 pp.

Klute, A. 1972. The determination of the hydraulic conductivity and diffusivity of unsaturated soils. Soil Science, v.113, no.4, pp.264-276.

Kessler, J. and R.J. Oosterbaan. 1974. Determining hydraulic conductivity of soils. In: Drainage Principles and Applications, v.3. Publ.16, International Institute for Land Reclamation and Improvement, P.O.Box 45, Wageningen, The Netherlands, pp.253-296.

Koorevaar, P., G. Menelik and C. Dirksen. 1983. Elements of Soil Physics. Elsevier. New York, N.Y. 228 pp.

Lee, D.M. 1984. A comparison of methods for measuring the saturated hydraulic conductivity of four field soils having a range of textures. M.Sc. Thesis, University of Guelph, Canada.

Lee, D.M., W.D. Reynolds, D.E. Elrick and B.E. Clothier. 1985. A comparison of three field methods for measuring saturated hydraulic conductivity. Canadian Journal of Soil Science, v.65, no.3, pp.563-573.

McWhorter, D.B., A.T. Corey and K.M. Adam. 1973. The elimination of trapped gas from porous media by diffusion. Soil Science, v.116, no.1, pp.18-25.

Nielsen, D.R., J.W. Biggar and K.T. Erh. 1973. Spatial variability of field-measured soil-water properties. Hilgardia, v.42, no.7, pp.215-259.

Parlange, J.Y. and W.L. Hogarth. 1985. Steady state infiltration: Consequences of α dependent on moisture content. Water Resources Research. v.21, no.8, pp.1283-1284.

Philip, J.R. 1968. Steady infiltration from buried point sources and spherical cavities. Water Resources Research, v.4, no.5, pp.1039-1047.

Philip, J.R. 1969. Theory of infiltration. Advances in Hydroscience, v.5; pp.215-296.

Philip, J.R. 1973. On solving the unsaturated flow equation: 1. The flux-concentration relation. Soil Science, v.116, no.5, pp.328-335.

Philip, J.R. 1985. Approximate analysis of the borehole permeameter in unsaturated soil. Water Resources Research. v.21, no.7, pp.1025-1033.

Reynolds, W.D. and D.E. Elrick. 1985. In-Situ measurement of field-saturated hydraulic conductivity, sorptivity and the α-parameter using the Guelph Permeameter. Soil Science (in press).

Reynolds, W.D. and D.E. Elrick. 1986. A method for simultaneous in-situ measurement in the vadose zone of field saturated hydraulic conductivity, sorptivity and the conductivity-pressure head relationship. Ground Water Monitoring Review. (in press)

Reynolds, W.D., D.E. Elrick and B.E. Clothier. 1985. The constant head well permeameter: Effect of unsaturated flow. Soil Science. v.139, no.2, pp.172-180.

Reynolds, W.D., D.E. Elrick and G.C. Topp. 1983. A reexamination of the constant head well permeameter method for measuring saturated hydraulic conductivity above the water table. Soil Science. v.136, no.4, pp.250-268.

Scotter, D.R., B.E. Clothier and E.R. Harper. 1982. Measuring saturated hydraulic conductivity and sorptivity using twin rings. Australian Journal of Soil Research, v.20, no.4, pp.295-304.

Snedecor, G.W. 1957. Statistical Methods Applied to Experiments in Agriculture and Biology. Iowa State College Press, Ames, Iowa. 534 pp.

Steel, R.G.D. and J.H. Torrie. 1980. Principles and procedures of statistics: A biometrical approach. McGraw-Hill, Toronto, Ont. 455 pp.

Stephens, D.B., K. Lambert and D. Watson. 1984. Influence of entrapped air on field determinations of hydraulic properties in the vadose zone. Proc. Conf. Characterization and Monitoring in the Vadose Zone. National Water Well Association., Worthington, pp.57-76.

Stephens, D.B., S. Tyler, K. Lambert and S. Yates. 1983. Field experiments to determine saturated hydraulic conductivity in the vadose zone. In: Role of the Unsaturated Zone in Radioactive and Hazardous Waste Disposal. J.W. Mercer (ed.). Ann Arbor Science. Ann Arbor, Mich., pp.113-126.

Talsma, T. 1965. Sample size estimates in permeability studies. Am. Soc. Civ. Eng. Proc. J. Irrig. and Drain. Div. 91, no.IR4:76-77.

Talsma, T. 1970. Some aspects of three-dimensional infiltration. Australian Journal of Soil Research, v.8, no.2, pp.179-184.

Topp, G.C. and M.R. Binns. 1976. Field measurement of hydraulic conductivity with a modified air-entry permeameter. Canadian Journal of Soil Science, v.56, no.3, pp.139-147.

Warrick, A.W. and D.R. Nielsen. 1980. Spatial variability of soil physical properties in the field. In Hillel, "Applications of Soil Physics". Academic Press. Toronto, Ont. pp.319-344.

Willardson, L.S. and R.L. Hurst. 1965. Sample size estimates in permeability studies. Am. Soc. Civ. Eng. Proc. J. Irrig. and Drain. Div. 91, no. IR1: 1-9.

Willett and P. H. Walker

soils recently reclaimed

National Soil Fertility

logy of some seasonally

soils: II. Production and

Soils', Vol. I, pp. 294-5.
n.)
potential of acid sulfate

forms of extractable iron

raktion mit Ammonium-

e of organic compounds
), Vol. I, pp. 645-55.
I.S. Government Printing

Mulcahy, M. J., and
S.A.)
rch 6, 90-3.
ds for Analysis of
Bur. Soils No. 54. (Com-

w area, Grafton, N.S.W.

ast of N.S.W. *J. Soil Sci.*

River, New South Wales.

in soils. *Aust. J. Soil Res.*

eoxidized rice soils. *Aust.*

rice growing on soil phos-

Aust. J. Soil Res., 1982, 20, 295-304

Measuring Saturated Hydraulic Conductivity and Sorptivity Using Twin Rings

D. R. Scotter[A], *B. E. Clothier*[B] *and E. R. Harper*[A]

[A] Department of Soil Science, Massey University, Palmerston North, N.Z.
[B] Plant Physiology Division, DSIR, Palmerston North, N.Z.

Abstract

A method of measuring, with minimal soil disturbance, the saturated hydraulic conductivity and sorptivity of field soil is presented and discussed. It involves measuring the steady-state infiltration of ponded water from two rings, of different radii, that have been lightly pressed into the soil surface. The method is based on Wooding's solution for steady infiltration from a shallow, circular pond. Criteria for selecting ring radii are discussed. Results for three field soils are found to give consistent values for the conductivity and sorptivity.

Introduction

Theory shows infiltration of ponded water into soil is largely dependent on two parameters, the sorptivity (S) and the saturated hydraulic conductivity (K) (Philip 1969). Infiltration is of interest in hydrological modelling and irrigation planning, so K and S values are useful. Two serious problems arise when field measurement of these parameters is attempted. Firstly S, and especially K, are very sensitive to any disturbance of the soil, as recent work on preferential flow in macropores (Bouma 1981) has highlighted. Existing methods of measuring K and S in the field involve driving a corer or ring into the soil, or augering out a cavity (Talsma 1969, 1970; Bouwer and Jackson 1974), so some compaction, fracturing or smearing almost inevitably occurs (Bouma and Dekker 1981). These disturbances must affect the measurement. Also existing methods are difficult or impossible to use in stony soils. The second problem is the large spatial variability of S (Sharma *et al.* 1980) and K (Warrick and Nielsen 1980), the coefficient of variation among replicate conductivity measurements often being greater than 100%.

Thus methods for measuring K and S should involve as little soil disturbance as possible, and be simple enough to allow adequate replication. The method described here goes some way towards meeting these criteria. It involves measuring the steady-state unconfined infiltration rate of ponded water from shallow rings of two different radii.

Theory

Steady Infiltration from a Circular Pond

Steady-state infiltration into uniform soil is described by (Philip 1969)

$$\nabla\cdot(D\nabla\theta) = \partial k/\partial z, \qquad (1)$$

where θ is the volumetric water content, z is depth (m), D the soil water diffusivity ($m^2\ s^{-1}$) and k the hydraulic conductivity ($m\ s^{-1}$). Usually both D and k depend

Enclosure 3
B.3.1.2.2.1

strongly on θ and the matric potential ψ (m). Equation (1) may be linearized using a parameter ϕ, termed the matric flux potential (Raats 1971) and defined as

$$\phi = \int_{\theta_n}^{\theta} D\,d\theta = \int_{\psi_n}^{\psi} k\,d\psi, \tag{2}$$

if the relationship between k and ψ is described by

$$k = K\exp(\alpha\psi). \tag{3}$$

In equation (2) θ_n is the water content prevailing before infiltration commences, and ψ_n is the corresponding value of ψ. In equation (3) α (m^{-1}) is a constant, and K again the hydraulic conductivity at effective saturation when $\psi = 0$.

Wooding (1968) solved equation (1), linearized as described, for the boundary condition of a shallow circular pond of radius r (m) on the soil surface. He noted a remarkable feature of the complex series solution that he obtained was that the flux density into the soil averaged over the source area, q ($m\ s^{-1}$), was almost identical with that given by the simple expression

$$q = \alpha\phi_s + 4\phi_s/(\pi r), \tag{4}$$

where

$$\phi_s = \phi(\theta_s) = \int_{\theta_n}^{\theta_s} D\,d\theta, \tag{5}$$

and θ_s is the water content at effective saturation. If the soil is initially at 'field capacity' or drier, $K \gg k(\theta_n)$ in most soils, so from equations (2) and (3) to a close approximation

$$\phi_s = K/\alpha. \tag{6}$$

Thus equation (4) may be rewritten as

$$q = K + 4\phi_s/(\pi r). \tag{7}$$

The two terms on the right-hand side of equation (7) have obvious physical significance. The first term is the steady-state solution for one-dimensional infiltration, while the second term is the solution for steady-state, gravity-free absorption from a shallow circular pond (Philip 1969). For large r the first term dominates and $q \equiv K$; for small r the second term is the more important and $q \equiv 4\phi_s/(\pi r)$. At intermediate values of r, equation (7) gives q simply as the sum of these two solutions. The pond radius r_e at which the two terms on the right-hand side of equation (7) are of equal magnitude is

$$r_e = 4\phi_s/(\pi K). \tag{8}$$

Equation (7) is only exact if equation (3) is exact. However, instead of being a constant, α is likely to be weakly dependent on ψ. An implication of work by Parlange (1972) is that the α used in equation (4) (defined more generally as $\alpha = (dk/d\theta)/D$) should then be the value pertaining at θ_n. Thus equation (6) will not be exact, and the value of K found not the true saturated hydraulic conductivity. However, the resulting error in K is likely to be small relative to the spatial and temporal variability of K in the field.

Solving for the Saturated Hydraulic Conductivity

Suppose two rings of radii r_1 and r_2 are used to pond water on the soil, and the resulting steady-state flux densities into the soil are q_1 and q_2 respectively. Solution of the simultaneous equations from equation (7) gives

$$K = (q_1 r_1 - q_2 r_2)/(r_1 - r_2). \tag{9}$$

To obtain reasonable sensitivity, it is desirable that $r_1 > 2r_2$ and r_1 be large enough for

$$C_K = (q_1 r_1 - q_2 r_2)/(q_1 r_1) > 0{\cdot}3, \tag{10}$$

where C_K is a dimensionless parameter defined by the above equation. C_K equals 0·3 if $r_1 = 2r_2$ and $r_e = (r_1 + r_2)/2$.

Owing to field variability, considerable replication is required when q is measured, as mean values are needed for use in equation (9). If the observed frequency distribution of q is approximately normal, an estimate of the standard error of K, $s(K)$, is given by (Barford 1967)

$$s(\overline{K}) = [(r_1 s_1)^2/n_1 + (r_2 s_2)^2/n_2]^{1/2}(r_1 - r_2)^{-1}, \tag{11}$$

where s_1 and s_2 are the standard deviations of q_1 and q_2 respectively, and n_1 and n_2 the number of replicate measurements.

However, both K and the sorptivity (S) have usually been found to approximate log-normal rather than normal distributions (Sharma *et al.* 1980; Warrick and Nielsen 1980) and q is likely to behave similarly. For a log-normally distributed variable X, the mean $\overline{X}$ is given by (Warrick and Nielsen 1980)

$$\overline{X} = \exp(\overline{X}_L + s_L^2/2), \tag{12}$$

where $\overline{X}_L$ and s_L are the mean and standard deviation respectively of the log-transformed variable $\ln(X)$. If fractile analysis shows q to be better described by a log-normal than a normal distribution, equation (12) can be used to obtain mean values of q_1 and q_2 for substitution into equation (9). In this case error theory (Barford 1967) suggests the standard deviation s may be approximated as

$$s = s_L \overline{q}, \tag{13}$$

giving values of s_1 and s_2 for use in equation (11).

Solving for the Sorptivity

Solving for the other unknown in the simultaneous equations referred to above gives the integral of the diffusivity function, ϕ_s, as

$$\phi_s = \left(\frac{\pi}{4}\right)(q_1 - q_2)/\left(\frac{1}{r_1} - \frac{1}{r_2}\right). \tag{14}$$

To obtain reasonable sensitivity from this equation, it is desirable that $r_1 > 2r_2$ again, and also that r_2 be small enough for

$$C_\phi = (q_2 - q_1)/q_2 > 0{\cdot}3, \tag{15}$$

where C_ϕ is a dimensionless parameter defined by the above equation. C_ϕ equals 0·3 if $r_1 = 2r_2$ and $r_e = (r_1 + r_2)/2$. An estimate of the standard error of ϕ_s, $s(\overline{\phi_s})$, is given by

$$s(\overline{\phi_s}) = \frac{\pi}{4}\left(\frac{1}{r_2} - \frac{1}{r_1}\right)^{-1}(s_1^2/n_1 + s_2^2/n_2)^{1/2}. \tag{16}$$

For a delta-function diffusivity, that is for a soil behaving as described by Green and Ampt (1911), the sorptivity is given by (Philip 1973)

$$S = [2\phi_s(\theta_s - \theta_o)]^{1/2}. \tag{17}$$

For a soil with a constant diffusivity independent of θ Philip (1969) showed that

$$S = [4\phi_s(\theta_s - \theta_o)/\pi]^{1/2}. \tag{18}$$

Equations (17) and (18) provide an envelope for the possible relationships between ϕ_s and S, and differ only by a factor of $(2/\pi)^{1/2}$ or 20%. As the diffusivity of most soils is better described using a delta-function than a constant value, the error

involved in using equation (17) to find S will usually be much less than 20%. Unless D is only weakly dependent on θ, or the pore geometry changes with θ, ϕ_s is relatively independent of θ_n. However, S is of course a function of θ_n, being approximately proportional to $(\theta_s-\theta_n)^{1/2}$, as equation (17) indicates. Ignoring errors induced by using equation (17) and the uncertainty in θ_s and θ_n, an estimate of the standard error of the sorptivity $s(S)$ is given by

$$s(\bar{S}) = [(\theta_s-\theta_n)/(2\phi_s)]^{1/2}s(\bar{\phi}_s). \quad (19)$$

Time to Reach Steady-State

For the above theory to be useful, q must approach the steady-state value within a reasonable time period. An analytical solution for transient infiltration from a circular pond is not available. While numerical solution is possible, it is complicated, expensive and not suitable for routine use. However, depending on whether the first or second term on the right-hand side of equation (7) is the larger, an estimate of the time required to approach steady infiltration may be found using the transient solutions for either one-dimensional infiltration or three-dimensional absorption. For this purpose the simple delta-function solutions (Philip and Knight 1974) should suffice.

For one-dimensional infiltration

$$t = \frac{S^2}{2K^2}\left[\frac{K}{q-K} - \ln\left(\frac{q}{q-K}\right)\right], \quad (20)$$

where t is time.

From equation (20) we find when $t = t^* = 1{\cdot}6(S/K)^2$, $q/q_\infty = 1{\cdot}2$, where t^* is a characteristic time when q is 20% higher than the steady-state value q_∞.

The transient three-dimensional absorption solution given by Philip and Knight (1974) applies to flow from a spherical cavity of radius r_0 rather than the shallow circular pond considered here. However, comparison of the steady-state solutions for these two boundary conditions and any $D(\theta)$ relation (Philip 1969) shows the flux density for a given radius only differs by a factor of $\pi/4$. The times to reach steady flow are probably also similar, particularly for relatively small radii. The delta function solution for absorption from a spherical cavity is (Philip and Knight 1974)

$$t = \frac{r_0^2(\theta_s-\theta_n)^2}{3S^2}\left\{1+2\left[1-\frac{S^2}{2qr_0(\theta_s-\theta_n)}\right]^{-3}-3\left[1-\frac{S^2}{2qr_0(\theta_s-\theta_n)}\right]^{-2}\right\}. \quad (21)$$

It follows that when $t = t^* = [10r_0(\theta_s-\theta_n)/S]^2$, equation (21) predicts $q/q_\infty = 1{\cdot}2$.

Materials and Methods

The proposed method was used at three sites (A, B and C) to measure K and S. K was also measured using two established methods. Two of the sites were alluvial soils of the Manawatu series (Dystric Fluventic Eutrocrepts), while site C, the Tokomaru silt loam (an Aeric Fragiaqualf), was a soil of loessial origin. Sites A and C were under pasture, while B was in a young apple orchard where regular herbicide application had kept the surface bare. At site A the texture was sandy loam to approximately 0·8 m, below which was fine sand. At site B the texture was fine sandy loam to 0·3 m, below which was medium to fine sand. At site C the silt loam topsoil changed to a light clay loam at 0·25 m. At sites A and B the top 20 mm of soil was removed before any measurements were made. At site C the surface was left intact.

Sharpened rings, with radii ranging from 0·025 to 0·204 m, were lightly pushed or gently driven approximately 10 mm into the soil, just far enough to prevent lateral leakage when water was ponded in them. Each ring was randomly located, with no two rings covering any common area. At site C it was found useful to cut through the vegetation with a knife where the cutting edge of the ring was to enter the soil, before inserting the ring. Alternatively, the rings may be cemented to the soil surface. A ponding depth of approximately 10 mm was used. The infiltration rate as a function of time was found either

using a calibrated Mariotte device, or more commonly the rings were refilled to a fixed level from a measuring cylinder at suitable time intervals, a matchstick being a suitable level indicator. Usually measurements were continued for an hour after steady-state appeared to have been reached. The volumetric water contents before infiltration commenced, and immediately after the ponded water had disappeared, were measured at each site.

K was also measured using the well-permeameter and field-core permeameter methods. The well-permeater method, subsequently referred to as the well method, involves measuring the steady infiltration from an auger hole in which a constant water level is maintained. The simplified procedure described by Talsma and Hallam (1980) was used, except that a 13 mm rather than 32 mm auger hole radius was used. This meant a hole only 140 mm deep was needed and measurement within the topsoil could be attempted. The field-core permeameter method, subsequently referred to as the core method, involved driving a 102 mm radius sharpened steel ring approximately 100 mm into the soil. The ring was dug out and the soil at the base chipped level. The core and ring were then stood on a perforated base, water ponded on the surface, and the flow rate measured when steady flow prevailed so that Darcy's law gave K.

Results and Discussion

K *Measurements*

Four ring radii were used at each site, and the resulting mean values of q and their standard deviations are shown in Table 1. At sites A and B fractile analysis (Warrick and Nielsen 1980) showed the frequency distributions to be somewhat better described by log-normal than normal distributions, so $\overline{q}$ and s were calculated using equations (12) and (13) respectively. At site C the distribution was closer to normal than log-normal, so q was calculated as the arithmetic mean and s was the usual standard deviation for a normal distribution.

Table 1. Infiltration data for rings

Soil	Measurement		r (m)	n[A]	$10^1\overline{q}$ (m/s)	$10^1 s$ (m/s)	T[B] (min)
A	I	r_1	0·180	10	1·2	0·4	30–70
		r_2	0·075	12	1·4	0·7	20–40
	II	r_1	0·102	20	1·4	0·5	20–50
		r_2	0·037	13	1·7	1·0	5–20
B	I	r_1	0·102	23	1·3	0·6	60–100
		r_2	0·037	14	3·0	3	30–50
	II	r_1	0·075	20	1·7	1·0	40–80
		r_2	0·025	13	3·7	3	5–30
C	I	r_1	0·204	4	1·7	0·5	40–80
		r_2	0·075	12	4·0	3	10–60
	II	r_1	0·102	25	3·2	1·0	20–50
		r_2	0·037	12	8·1	3	10–30

[A] Number of measurements.
[B] T is the range of times elapsed until q appeared steady.

The average coefficient of variation of q was 40% at sites A and C and 70% at site B. The higher variability at site B was apparently related to the texture change at 0·3 m depth. This may have induced instability at the wet front (Hill and Parlange 1972), although this would probably not affect the surface flux very much. It is more likely that the layering enhanced the effect of worm holes in the A horizon and so on q. Cracks and worm holes are of finite length, so while they initially have a dominating influence on infiltration from a pond, they usually have much less influence on steady infiltration. At site B, however, worm holes from the surface to the sand B horizon were observed to short-circuit the less-permeable A horizon, and so significantly increase the value of q found with particular rings.

The four ring radii at each site were treated as two pairs (I and II), allowing two independent calculations of K and ϕ_s to be made. The ring pairings were selected so $r_1 > 2r_2$ in all cases. The resulting K values and their standard errors are shown as the ring data in Table 2. Also shown is C_K. At site A, C_K is largest, and $s(\overline{K})$ is relatively small. At site B, $C_K \equiv 0{\cdot}3$, and this, coupled with the higher variability of q at this site, causes the standard error to be the same order of magnitude as K. Larger rings and/or more measurements would have been needed to obtain a more accurate estimate of $\overline{K}$. At site C, $C_K < 0{\cdot}3$, and again $\overline{K}$ and $s(\overline{K})$ are of similar magnitude; here again larger rings would have been needed to obtain an accurate estimate of $\overline{K}$.

Table 2. Saturated hydraulic conductivity data

Soil	Measurement	$\overline{K}$ (m/s)	$s(\overline{K})$ (m/s)	C_K	n
A	Ring I	$1{\cdot}0\times10^{-5}$	3×10^{-6}	0·5	–
	Ring II	$1{\cdot}2\times10^{-5}$	2×10^{-6}	0·6	–
	Well	$2{\cdot}1\times10^{-6}$	2×10^{-7}	–	18
	Core	$8{\cdot}3\times10^{-6}$	2×10^{-6}	–	20
B	Ring I	$3{\cdot}1\times10^{-6}$	3×10^{-6}	0·2	–
	Ring II	$7{\cdot}3\times10^{-6}$	5×10^{-6}	0·3	–
	Well	$1{\cdot}2\times10^{-6}$	2×10^{-7}	–	20
	Core	$7{\cdot}7\times10^{-5}$	3×10^{-5}	–	13
C	Ring I	$4{\cdot}0\times10^{-6}$	4×10^{-6}	0·2	–
	Ring II	$4{\cdot}6\times10^{-6}$	6×10^{-6}	0·1	–
	Well	$3{\cdot}4\times10^{-7}$	5×10^{-8}	–	12
	Core	$3{\cdot}1\times10^{-5}$	7×10^{-6}	–	23

The $\overline{K}$ and $s(\overline{K})$ values found using the well method are also shown in Table 2. The distributions at sites A and B were slightly nearer log-normal than normal, while at site C the distribution was nearer to normal. In all cases the well K values are lower than the ring values, at site A significantly so ($P < 0{\cdot}01$ by t-test). However, the well method is not really suited to measurements near the surface, and the small well-radius used, coupled with smearing and sealing of macropores at the well wall, probably induced systematic error in these measurements.

The data obtained using the core method also appear in Table 2. In this case at all three sites the frequency distributions were well described by log-normal distributions, but very poorly described by normal distributions. The few high K values causing the asymmetric distributions were probably for cores in which there was flow through vertical channels or cracks (Bouma 1981). To what extent these macropores were natural features, or were induced during core-ring insertion, is not known. However, in either case they probably induce systematic error, as *in situ* macropores would tend to have restricted continuity compared to the same macropores in a core. The K values obtained at site A using the ring and core methods were similar, although at the other two sites the core values were at least an order of magnitude greater than the ring values. At all three sites the core values were significantly higher than the well values. This contrasts with the agreement between the two methods found by Talsma and Hallam (1980) from measurements at 0·3–0·6 m depth, using similar-sized cores. The New Zealand topsoils studied here would probably have been more biologically active, and wetter when sampled, than the Australian subsoils studied by Talsma and Hallam. Thus the effects of smearing when using the well method, and of short-circuiting when using the core method, would probably be greater in the New Zealand topsoils than in Australian subsoils.

S *and* ϕ_s *Measurements*

The ϕ_s and sorptivity data (calculated using equation (17)) obtained from the ring method are given in Table 3. For ϕ_s the reverse of the situation with K applies; good measurements of ϕ_s were obtained at site C, where $C_*>0{\cdot}3$, but at site A, $C_*<0{\cdot}3$ and $s(\overline{\phi_s})$ is the same order of magnitude as ϕ_s. Rings of radius less than 0·037 m would have been needed at site A to obtain a more accurate measure of ϕ_s. At site B, $C_*>0{\cdot}3$, but $s(\overline{\phi_s})$ is about half of ϕ_s owing to the high variability of q at this site.

Using different ring radii there is close agreement between the two independent measurements of K at site A and ϕ_s at site C. This is reassuring. It confirms that equation (7) can be used to describe the relationship between q and r. Also it suggests that the q values obtained were close to steady-state, otherwise the different transient responses with the different ring radii would probably have resulted in inconsistent K and ϕ_s values. Transient behaviour is discussed further in the following section.

Table 3. Sorptivity and ϕ_s data from rings

Soil	Measurement	$10^7 \times \phi_s \pm s(\overline{\phi_s})$ ($m^2\ s^{-1}$)	C_*	$10^4 \times [S \pm s(\overline{S})]$ ($m\ s^{-1/2}$)	r_2 (m)
A	I	2·0±3	0·1	3·5±3	0·03
(θ_s=0·43) (θ_a=0·12)	II	1·3±1	0·2	2·9±1	0·01
B	I	7·7±4	0·6	6·0±2	0·3
(θ_s=0·43) (θ_a=0·20)	II	5·8±3	0·5	5·2±1	0·1
C	I	21±2	0·6	8·2±0·4	0·7
(θ_s=0·46) (θ_a=0·30)	II	22±5	0·6	8·4±1	0·6

Values for r_2 at each site are also given in Table 3. As r_2 should be between r_1 and r_2 if it is desired to find both K and S from one set of measurements, the range of r_2 from 0·01 m to 0·7 m shows different ring radii will be optimal in different soils. However, values of $r_1 = 0{\cdot}5$ m and $r_2 = 0{\cdot}025$ m would be suitable for many soils.

Transient Behaviour

One problem with the proposed method is that it depends on steady-state infiltration being attained. This can take many hours in some situations (Bond and Collis-George 1981). For example, t^* for one-dimensional infiltration was 14 h for the Glebe loam soil characterized by Talsma (1970). Futhermore, infiltration may appear to be steady long before it has reached its final value, although plotting q against $\log(t)$ rather than t can help avoid a premature assumption of steady-state.

In Fig. 1, q is shown as a function of time for two 0·18 m radius rings at site A. After 10 min the change in q is small relative to the resolution of the measurement and very small compared with differences between the q values for the duplicate rings. In this case the first term on the right-hand side of equation (7) dominates, so equation (20) gives the better indication of the expected transient behaviour. As seen in Fig. 1, the resulting curve (calculated using average values of S and K) and the ring data show similar transient behaviour; also $t^* = 23$ min, in line with the observed elapsed times for q to appear steady of 30–70 min (Table 1). As is also illustrated in Fig. 1, the wetter the soil before infiltration commences, the more

quickly steady infiltration is approached, the higher θ_n values lowering S. Despite its smaller contribution to q, the three-dimensional absorption solution (equation (21)) shown in Fig. 1 has a greater absolute transient error after 100 min than equation (20) with $t^* = 35$ days. But this is an overestimate of the error in this case, as the two solutions will interact during the transient phase, gravity wetting the soil below the rings much more quickly than would absorption alone.

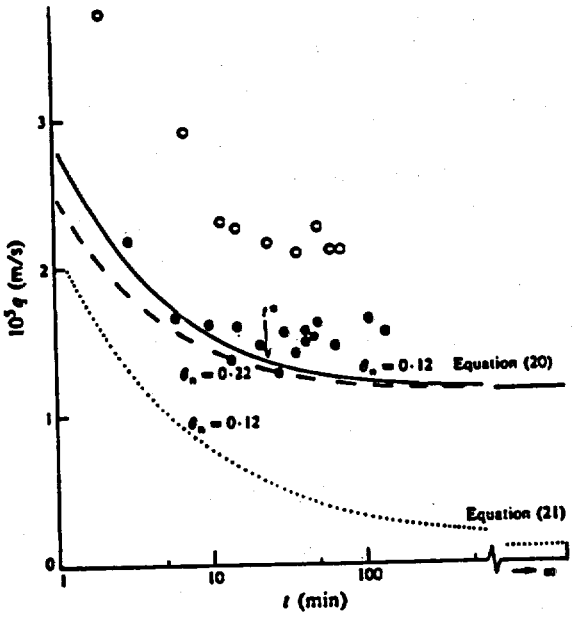

Fig. 1. Observed changes of q with time after the initiation of ponding for two 0·18 m radius rings at site A (○ and ●). Also shown are curves from equations (20) and (21) and values of t^* and q_∞, calculated using average values of K, ϕ_s and θ_s measured with the rings at that site.

The calculated transient behaviour for 0·037 m radius rings at site B, shown in Fig. 2, contrasts with the data in Fig. 1. In this case the second term on the right-hand side of equation (7) makes the dominant contribution to q. Equation (21) predicts $t^* = 380$ min, but owing to interaction with the first term this is probably an overestimate. Again, a higher θ_n hastens the approach to steady-state, as is shown in the Figure. The values for T in Table 1 indicate that q appeared to be steady after 30–50 min, that is, systematic change in q during the subsequent hour was not detectable. As the plot of the solution to equation (21) in Fig. 2 shows, this does not mean a true steady-state had been reached, but compared to other uncertainties affecting the measurement of q in the field, non-steady behaviour should not be a serious problem in many soils. In the soils studied here q approached steady-state within 1–3 h, although in initially drier, poorly structured or swelling soils much longer times may be involved.

The experimental transient behaviour shown in Fig. 2 for two rings at site B is in general agreement with the calculated transient response, except that after 120 min q in one ring suddenly doubled. This is thought to be due to an earthworm suddenly venting its burrow to the surface; ponding tends to encourage such activity. Also the presence of a sandy horizon below 0·3 m depth probably tended to enhance the effect on infiltration of worm holes and other macropores, which could short-circuit the less permeable topsoil. This could also explain the higher coefficient of variation in q at this site. While exceptional, the sudden increase shown is a dramatic illustration of temporal variation in q, and so K and S.

Limitations of the Method and Variability of K *and* ϕ_s

The results obtained using the proposed method may be invalid or need careful interpretation in particular situations. If the soil surface has a low conductivity crust the theory outlined here will not apply, but other simple theory will (Hillel 1971). If the hydraulic conductivity is anisotropic, as found for example by Bouma and Dekker (1981), the proposed method will tend to measure the vertical rather than the horizontal conductivity. On the other hand, the well method tends to measure K mainly in the horizontal direction (Bouwer and Jackson 1974), and this is another reason why results using the two methods may not agree. Also, as discussed in the previous section, a steady-state value of q may not be attainable in some soils, making the proposed method difficult or impossible to use.

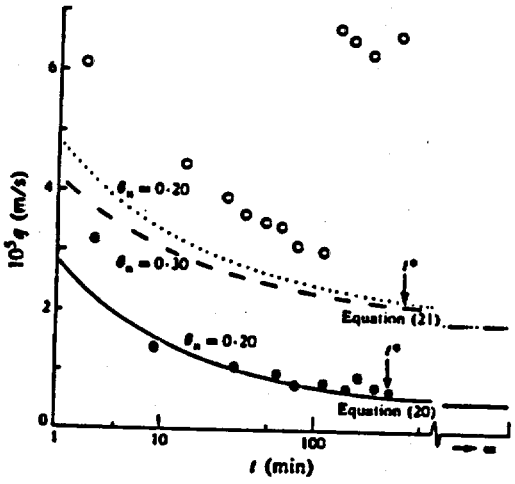

Fig. 2. Observed changes in q with time for two 0·037 radius rings at site B (O and ●). Also shown are curves from equations (20) and (21) and values of t^* and q_∞, calculated using average values of K, ϕ_s and θ_s measured with the rings at that site.

The reason for measuring K and S in the field is usually to explain or predict the long-term hydrological behaviour of the soil in a catchment or agricultural area. This involves considerable extrapolation of the data in both time and space. Spatial variability of K and S has been studied recently, but perhaps not enough attention has been paid to temporal variability.

A sudden change in K and S is described in the previous section. More gradual, but nevertheless significant, changes in K and ϕ_s in the topsoil with season or soil management will also occur. Just the effect of temperature on the viscosity of water will cause K to increase 70% if the soil temperature changes from 5 to 25°C. Most of the larger pores in the topsoil of finer-textured soils are induced biologically, or by shrinking and swelling as the soil wets and dries. Also imposed stresses, such as compaction, cultivation or the removal of vegetation, can alter the pore geometry. The macropore geometry is thus continually changing. As ϕ_s, and particularly K, are so sensitive to even slight changes in the larger soil pores and their continuity, these parameters are also subject to change. This should be remembered when extrapolating values measured at a particular site on a particular day.

Conclusions

The method of measuring K and S described is simple. It needs a minimum of equipment and effort, thus allowing adequate replication of measurements. The method also minimizes soil disturbance and associated systematic errors in K due to

seem to be particularly useful where values of K and S are needed for infiltration studies related to hydrology or irrigation.

The theory on which the method is based assumes that steady infiltration occurs into a soil uniform with depth. In the field, soil is not uniform with depth and truly steady infiltration from water ponded in a ring probably never occurs. However, in comparison with uncertainty due to spatial and temporal variability of K and S, errors due to the assumptions of the theory not being met are probably insignificant in many situations.

References

Barford, N. C. (1967). 'Experimental Measurements: Precision, Error and Truth.' (Addison-Wesley: London.)

Bond, W. J., and Collis-George, N. (1981). Ponded infiltration into simple soil systems: 3. The behaviour of infiltration with time. *Soil Sci.* 131, 327-33.

Bouma, J. (1981). Soil morphology and preferential flow along macropores. *Agric. Water Manage.* 3, 235-50.

Bouma, J., and Dekker, L. W. (1981). A method for measuring the vertical and horizontal K_{sat} of clay soils with macropores. *Soil Sci. Soc. Am. J.* 45, 662-3.

Bouwer, H., and Jackson, R. D. (1974). Determining soil properties. *In* 'Drainage for Agriculture', ed. J. van Schilfgaarde, pp. 611-72. (Am. Soc. Agron.: Madison, Wisc.)

Green, W. H., and Ampt, G. A. (1911). Studies in soil physics. I. The flow of air and water through soils. *J. Agric. Sci.* 4, 1-24.

Hill, E. D., and Parlange, J-Y. (1972). Wetting front instability in layered soils. *Soil Sci. Soc. Am. Proc.* 36, 697-702.

Hillel, D. (1971). 'Soil and Water: Physical Principles and Processes.' (Academic Press: New York.)

Parlange, J-Y. (1972). Theory of water movement in soils: 4. Two and three dimensional steady infiltration. *Soil Sci.* 113, 96-101.

Philip, J. R. (1969). Theory of infiltration. *Adv. Hydrosci.* 5, 215-96.

Philip, J. R. (1973). On solving the unsaturated flow equation: 1. The flux-concentration relation. *Soil Sci.* 116, 328-35.

Philip, J. R., and Knight, J. H. (1974). On solving the unsaturated flow equation: 3. New quasi-analytical technique. *Soil Sci.* 117, 1-13.

Raats, P. A. C. (1971). Steady infiltration from point sources, cavities and basins. *Soil Sci. Soc. Am. Proc.* 35, 689-94.

Sharma, M. L., Gander, G. A., and Hunt, C. G. (1980). Spatial variability of infiltration in a watershed. *J. Hydrol.* 45, 101-22.

Talsma, T. (1969). *In situ* measurement of sorptivity. *Aust. J. Soil Res.* 7, 269-76.

Talsma, T. (1970). Some aspects of three-dimensional infiltration. *Aust. J. Soil Res.* 8, 179-84.

Talsma, T., and Hallam, P. M. (1980). Hydraulic conductivity measurement of forest catchments. *Aust. J. Soil Res.* 18, 139-48.

Warrick, A. W., and Nielsen, D. R. (1980). Spatial variability of soil physical properties in the field. *In* 'Applications of Soil Physics', ed. D. Hillel, pp. 319-44. (Academic Press: New York.)

Wooding, R. A. (1968). Steady infiltration from a shallow circular pond. *Water Resour. Res.* 4, 1259-73.

Manuscript received 18 December 1981, accepted 5 May 1982

version

DRAFT

Brady rvw
04/12/91

PRECIPITATION ESTIMATION IN MOUNTAINOUS TERRAIN USING MULTIVARIATE GEOSTATISTICS: 2. ISOHYETAL MAPS

SUM-BSP
6-20-01

By Joseph A. Hevesi[1], Alan L. Flint[2] and Jonathan D. Istok[3]

[1]Geologist, Raytheon Services Nevada, Las Vegas, Nevada
[2]Hydrologist, U.S. Geological Survey, Mercury, Nevada
[3]Associate Professor, Dept. of Civil Engineering, Oregon State University, Corvallis, Oregon

Technical Journal for

JOURNAL OF APPLIED METEOROLOGY

Enclosure 3
8.3.1.2.2.1

(FOR REVIEW PURPOSES ONLY)

Table of Contents

PRECIPITATION ESTIMATION IN MOUNTAINOUS TERRAIN USING MULTIVARIATE GEOSTATISTICS: 2. ISOHYETAL MAPS

Joseph A. Hevesi
Raytheon Services Nevada
Las Vegas, Nevada

Alan L. Flint
U. S. Geological Survey
Mercury, Nevada

Jonathan D. Istok
Associate Professor
Department of Civil Engineering
Oregon State University
Corvallis, Oregon

April 5, 1991

LIST OF TABLES

DIRECTED

LIST OF FIGURES

PRECIPITATION ESTIMATION IN MOUNTAINOUS TERRAIN USING MULTIVARIATE GEOSTATISTICS: 2. ISOHYETAL MAPS

ABSTRACT

Values of average annual precipitation (AAP) may be important for hydrologic characterization of a potential high-level nuclear waste repository site at Yucca Mountain, Nevada. Reliable measurements of AAP are sparse in the vicinity of Yucca Mountain, and estimates of AAP were needed for an isohyetal mapping over a 2,600 mi^2 watershed containing Yucca Mountain. Estimates were obtained with a multivariate geostatistical model developed using AAP and elevation data from a network of 42 precipitation stations in southern Nevada and southeastern California. An additional 1,531 elevations were obtained to improve estimation accuracy. Isohyets representing estimates obtained using univariate geostatistics (kriging) defined a smooth and continuous surface. Isohyets representing estimates obtained using multivariate geostatisitcs (cokriging) defined an irregular surface that more accurately represented expected local orographic influences on AAP. Cokriging results included a maximum estimate within the study area of 335 mm at an elevation of 7,400 ft, an average estimate of 157 mm for the study area, and an average estimate of 172 mm at 8 locations in the

vicinity of the potential repository site. Kriging estimates tended to be lower in comparison because the increased AAP expected for remote, mountainous topography was not adequately represented by the available sample. Regression results between cokriging estimates and elevation were similar to regression results between measured AAP and elevation. The position of the cokriging 250 mm isohyet relative to the boundaries of pinyon pine and juniper woodlands provided indirect evidence of improved estimation accuracy because the cokriging result was in good agreement with investigations by others concerning the relationship between elevation, vegetation, and climate in the Great Basin. Calculated estimation variances were also mapped and compared to evaluate improvements in estimation accuracy. Cokriging estimation variances were reduced by an average of 54% relative to kriging variances within the study area. Cokriging reduced estimation variances at the potential repository site by 55% relative to kriging. The usefulness of an existing network of stations for measuring AAP within the study area was evaluated using cokriging variances, and twenty additional stations were located for the purpose of improving the accuracy of future isohyetal mappings. Using the expanded network of stations, the maximum cokriging estimation variance within the study area was reduced by 78% relative to the existing network, and the average estimation variance was reduced by 52%.

1. Introduction

Yucca Mountain, Nevada, is a potential location for a high-level nuclear waste

repository. The conceptual perimeter drift boundary for the potential repository site is an area of approximately 2 mi^2 beneath the southern extent of Yucca Mountain. The location was selected for a potential repository site partly because of a sparsity of percipitation. Values of average annual precipitation (AAP) are desired for hydrologic studies concerning site characterization, such as water-budget analyses, ground-water flow modeling, and the characterization of current climatic conditions. Unfortunately, reliable measurements of AAP are sparse in the vicinity of Yucca Mountain. Estimates of AAP can be calculated using more reliable measurements from surrounding precipitation stations in southern Nevada and southeastern California. Previous estimates of AAP at Yucca Mountain have ranged from 100 to 150 mm/yr (Winograd and Thordarson 1975; Quiring 1983). Montazer and Wilson (1984) used an estimate of 150 mm AAP to help estimate net infiltration at Yucca Mountain. An estimate of recharge, based on an AAP value of 150 mm, was calculated by Czarnecki (1985) in a model of groundwater flow of Yucca Mountain and vicinity.

This article presents the first application of multivariate geostatistical methods to the problem of estimating AAP at Yucca Mountain and the surrounding Upper Amargosa River Watershed (UARW), an area of approximately 2,600 mi^2 centered on the potential repository site (Fig. 1). Yucca Mountain is located in the northern Amargosa desert of southern Nevada, along the transitional boundary of the Great Basin Desert to the north and the Mojave Desert to the south (McMahon, 1985). The UARW is within the southern Basin and Range physiographic province, and includes most areas considered important for a hydrologic characterization of the potential repository site.

Elevations for the mountainous terrain within the watershed range from a minimum of 2,000 ft to a maximum of 7,694 ft. A more complete description of the physiography and climate of the UARW are in Hevesi et al. (19XX).

Orographic effects caused by mountainous terrain can result in a significant positive correlation between AAP and station elevation. Dingman et al. (1988) used an "elevation scale factor" to remove an observed orographic influence of elevation on AAP in Vermont and New Hampshire. Quiring (1983) and French (1986) fit regression equations between AAP and station elevation for precipitation stations in southern Nevada and southeastern California. Hevesi et al. (19XX) used data from 42 precipitation stations in southern Nevada and southeastern California to compute a correlation coefficient (r) of 0.75 between the natural log of AAP and station elevation.

In this article, variogram models defined by Hevesi et al (19XX) were used to prepare 2 isohyetal maps of AAP for the UARW. The first map was prepared using estimates calculated with AAP data (kriging). The second map was prepared using estimates calculated with both AAP and elevation data (cokriging). The usefulness of the maps for characterizing AAP within the UARW was evaluated. The effectiveness of applying a multivariate geostatistical model, using a large sample of elevation to obtain improved estimates of AAP, was evaluated by mapping the differences in cokriging and kriging estimates and by mapping the reductions in estimation variances of cokriging relative to kriging.

The AAP-elevation correlation represented by the geostatistical model was validated using regression between estimated values of AAP and known elevations. The

regression results for the estimates were compared with regression results between measured values of AAP and elevation. An independent validation of the results was made by comparing the location of the estimated 250-mm isohyet with the location of boundaries defining the occurrence of pinyon pine and juniper woodlands within the UARW.

Cokriging estimation variances were calculated for the active precipitation network to determine the effectiveness of this network for future isohyetal mappings of AAP within the UARW. To analyze the potential effectiveness of an expanded network of precipitation stations, locations for 20 additional stations were selected by computing cokriging estimation variances for the existing network and identifying the locations of maximum estimation variances within the UARW.

2. Methodology

a. Precipitation and Elevation Data

Measured values of AAP from 42 precipitation stations in the southern Nevada and southeastern California region were obtained for estimating AAP (Fig. 1). The lengths of record for these stations ranged from 8 to 53 years (Table 3, Hevesi et al., 19XX). The use of measurements from stations with relatively short lengths of record was necessary to obtain a sample large enough for a geostatistical analysis. The nearest station to the potential repository site (station 75, AAP = 119 mm) was located

approximately 10 mi ESE and the farthest station (station 225, AAP = 115 mm) was located approximately 140 mi WNW. The sample did not include stations located on Yucca Mountain because the length of record for these stations was less than 8 years at the time of this study. Ten of the 42 selected stations were within the boundaries of the UARW (Fig. 1). Station elevations were combined with 1,531 elevations recorded from topographic maps using a square grid with a spacing of 10,000 ft. This density was considered sufficient for preparing isohyetal maps of AAP for the UARW. Elevations for the grid locations ranged from -250 to 8,400 ft. The grid was centered on the UARW and included a total of 747 locations within the UARW (Fig. 2, Hevesi, et al., 19XX).

b. Estimating Average Annual Precipitation (AAP)

Estimates and estimation variances were calculated using ordinary kriging and cokriging (Journel and Huijbregts, 1978). The variogram models selected by Hevesi et al. (19XX) were defined in terms of a transformed variable, TAAP, where TAAP = ln(AAP)*1000, because the 42 AAP measurements approximated a log-normal distribution, and the linear geostatistical methods used in this study required the data to be normally distributed (Journel and Huijbregts 1978). To provide minimum cokriging estimation variances, the variogram models were used to calculate estimates and estimation variances for TAAP at the same 1,531 grid locations used to obtain the elevation sample. The method of sliding neigborhoods was used to calculate each

estimate within a circular search neighborhood because the variogram models were defined using the assumption of quasi-stationarity (Journel and Huijbregts 1978). Separate radii for the two search neighborhoods for TAAP and elevation were needed because of the inconsistent spatial distributions between the TAAP and elevation samples. Estimates were also calculated for 10 precipitation stations located within the UARW that were operational at the time of this study but were not included in the sample of measured AAP because of lengths of record less than 8 years (Table 1). Eight of these stations were located on Yucca Mountain, in the vicinity of the potential repository site.

To compute estimates and estimation variances for AAP, inverse transformations were made using the following equations (Cooper and Istok, 1988):

$$AAP^*(x_o) = K_o \exp[\, TAAP^*(x_o)/1000 + \sigma_k^2(x_o)/1{,}000{,}000 \,] \quad (1)$$

$$\sigma^2_{AAP}(x_o) = m^2[\, \exp(\sigma^2)(1-\exp(\sigma_k^2(x_o)/1{,}000{,}000)) \,] \quad (2)$$

$$K_o = \left(\frac{1}{n} \sum_{i=1}^{n} TAAP^*(x_o) \,/\, 1000 \right)/m \quad , \quad (3)$$

where $AAP^*(x_o)$ is the estimate for AAP at the point x_o, $TAAP^*(x_o)$ and σ_k^2 are the estimate and estimation variance for TAAP obtained using kriging or cokriging, n is the sample size, m is the sample mean for AAP, σ^2_{AAP} is the estimation variance for AAP,

and σ^2 is the sample variance for TAAP. The parameter K_o is used to correct for bias in the inverse transformation.

c. Evaluation of Isohyetal Mappings

The transformed kriging and cokriging estimates were mapped using isolines to represent the values calculated at the 1,531 grid locations (isohyets are isolines of AAP). The general characteristics of the kriging and cokriging isohyetal mappings were visually compared to evaluate the influence of the elevation sample on estimates of AAP. The values and locations of maximum and minimum estimates within the UARW, and the values of estimates at the 8 precipitation stations in the vicinity of the potential repository site, were identified. Global (area averaged) estimates for AAP were obtained by computing the arithmetic average of AAP estimates for points within the UARW (Istok and Cooper, 1988). A direct comparison of the two isohyetal mappings was made by mapping the difference between cokriging and kriging estimates. An evaluation of estimation accuracy was made by a visual inspection of the mapped estimation variances, and a comparison of relative estimation accuracy was made by mapping the percent reduction in cokriging variances relative to the kriging variances.

d. Validating Kriging and Cokriging Estimates

Estimates were calculated for the same 1,531 grid locations used to obtain the

elevation sample, and this configuration permitted a regression analysis between estimated AAP and measured elevation. Regression results obtained between estimated AAP and elevation were compared with results obtained between measured AAP and elevation (Hevesi et al, 19XX). The comparison was used to evaluate the geostatistical model's performance in terms of preserving the AAP-elevation correlation observed in the southern Nevada region. and also to compare estimates obtained using the geostatistical model with estimates obtained using only elevation data and fitted regression equations.

For the purpose of obtaining an independent validation, the location of the estimated 250-mm isohyet was compared with the boundaries of sparse to moderately vegetated pinyon pine and juniper woodlands identified on topographic maps, areal photographs, and in the field. The occurence of these woodlands in the UARW and vicinity was observed to be correlated with high elevations of approximately 6,000 ft and above that receive relatively high precipitation and have low air temperatures. The boundaries did not include low elevation woodlands resulting from the occurrence of springs or a shallow water table.

The selection of the 250-mm isohyet was based partly on observations by Houghton, et al (1975) concerning the relation between elevation, climate, and the distribution of plant communities in the Great Basin. Their results indicated a correlation between an elevation of 5,900 ft, an AAP value of 250 mm, and the approximate lower limit for the occurence of pinyon pine and juniper woodlands, defining the boundary between a moist steppe and a dry steppe climate in the Great

Basin. The selection of the 250-mm isohyet was also based on the observation that, from the sample of 42 precipitation stations used in this study, all 6 measurements of AAP greater than 250 mm were at elevations greater than 6,000 ft (Fig. 4, Hevesi, et al, 19XX), and were located within or directly adjacent to woodland boundaries. Unpublished investigations on the relations between elevation, AAP, and plant communities in the southern Nevada region substantiated 250 mm as a reasonable value to be correlated with the occurence of pinyon pine and juniper woodlands (John Emerick, oral communication, 1990).

provide association (Govt agency/academic institution/private enterprise)

d. Using Estimation Variances to Evaluate the 1990 Network

The 42 precipitation stations used to develop geostatistical models and isohyetal maps of AAP included 28 stations that were still operational in 1990 and actively collecting data at the time of this study. An additional 10 stations within the UARW that were not used for model development and estimation because of lengths of record less than 8 years were also active at the time of this study. Eight of the 10 stations were located on Yucca Mountain. A summary of the data for the total network of 38 active stations is in Table 1.

Assuming that sufficient lengths of record would be available in the future for obtaining reliable measurements of AAP at the 38 locations, the effectiveness of the network for characterizing AAP within the UARW was evaluated by mapping the cokriging estimation variances. Cokriging was applied using the 38 known locations and

arbritrary, or "fictitious" values of AAP. The selected values for AAP were arbitrary because only the variogram models and data locations were needed to calculate estimation variances (Journel and Huijbregts, 1978). In this study the selected values consisted of the 28 measured values and 10 fictitious values of AAP for the stations with lengths of record less than 8 years (Table 1).

e. Identifying Locations for Additional Precipitation Stations

An investigation of potential improvements in characterizing AAP for the UARW by expanding the existing network was made using cokriging estimation variances. Begining with the results obtained for the existing network of 38 active stations, the location for an additional precipitation station was selected by identifying the grid location with the maximum cokriging estimation variance within the UARW. The coordinates of that location were then added to the available data, and the procedure of calculating estimation variances was repeated to identify the location for the next station. The value of AAP used for each additional station was arbritrary because only the estimation variances were considered in this procedure. Locations for a total of 20 additional, or "fictitious", precipitation stations were identified, and the reductions in maximum and average estimation variance for the UARW obtained using the expanded network of 38 active and 20 fictious stations were analyzed.

3. Results and Discussion

a. Evaluation of Isohyetal Mappings

The kriged isohyets defined a smooth surface that indicated a gradual increase in AAP from the southwest to northeast across the UARW (Fig. 2a). Orographic effects were indicated only as a general trend of increasing AAP towards the northeastern edge of the watershed. Kriging estimates exceeding 250 mm were obtained for one area in the northeast section of the UARW and included 1.9% of the total area within the watershed (Table 2). Estimates of less than 100 mm included 11.4% of the watershed area and occurred in the Amargosa Desert and the Funeral Mountains. A maximum estimate of 287 mm was calculated for an elevation of 7,500 ft on Pahute Mesa, close to the northeastern edge of the watershed boundary, and a minimum estimate of 86 mm was obtained at an elevation of 5,000 ft in the Funeral Mountains (Table 2). A global estimate of 142 mm was calculated for the total area of the UARW. Kriged estimates at the locations of the 8 precipitation stations on Yucca Mountain ranged from 160 to 130 mm (Table 3). An average estimate of 143 mm AAP was obtained for these 8 stations located in the close vicinity of the potential repository site.

The cokriging isohyets defined an irregular surface that was similar to the known topography, indicating a strong influence of the elevation data on the calculated

(1) Table 2 average is 145 mm. Is the average supposed to be different from the global?

estimates (Fig. 3a). Estimates exceeding 250 mm were calculated for 5.2% of the UARW (Table 2) and included several areas within the watershed; the Grapevine Mountains, the Spring Mountains, Timber Mountain, Shoshone Mountain, and the northern part of Yucca Mountain. Estimates less than 100 mm were obtained for locations in the southern Amargosa Desert and included 9.2% of the watershed area. A maximum estimate of 335 mm was obtained at an elevation of 7,400 ft on Pahute Mesa, and a minimum estimate of 79 mm was obtained at an elevation of 2,200 ft for a location in the southern Amargosa Desert (Fig 3a, Table 2). The global estimate calculated for the UARW was 157 mm, 12 mm greater than the kriging global estimate. Cokriging estimates for the 8 stations on Yucca Mountain ranged from 145 mm at an elevation of 3,750 ft to 247 mm at an elevation of 5,870 ft (Table 3), representing a maximum gradient of 48 mm AAP per 1000 ft elevation in the vicinity of the potential repository site. An average cokriging estimate of 172 mm was obtained for these 8 stations, a 29 mm increase relative to the average kriging estimate. The maximum cokriging estimate of 247 mm was 87 mm greater than the maximum kriging estimate at Yucca Mountain. In general, significant orographic effects in the vicinity of the potential repository site were indicated by the cokriging estimates, but not by the kriging estimates, because increased AAP at the higher elevations on Yucca Mountain were not adequately represented by the available sample of 42 AAP measurements.

Contours of the quantity: "cokriging AAP estimate - kriging AAP estimate" conformed to contours of elevation; large positive values (cokriging estimates exceeding kriging estimates) occurred along the crests of mountain ranges whereas negative values

occurred in the basins and valleys (Fig. 4). The largest values occurred in areas of high local relief and in areas farthest from the precipitation stations. Within the UARW, cokriging estimates were 100 mm greater than kriging estimates at the Grapevine Mountains, the Funeral Mountains, the Spring Mountains, and Timber Mountain, because of a lack of AAP measurements at the higher elevations of these remote and mountainous locations. Cokriging estimates were 20 mm smaller than the kriging estimates at Yucca Flat, Sarcobatus Flat, and in the southern section of the Amargora Desert. Cokriging estimates for elevation grid locations at Yucca Mountain were 20 to 80 mm greater than kriging estimates, depending on elevation.

b. Comparison of Kriging and Cokriging Estimation Variances

Kriging and cokriging estimation variances indicated similar trends in estimation accuracy throughout the UARW; small values near the cluster of stations on the Nevada Test Site (NTS, Fig. 1) indicated relatively high estimation accuracy and large values at the southern, western, and northern boundaries of the watershed indicted areas of relatively low estimation accuracy (Figs. 2b, 3b). The locations of maximum and minimum estimation variances were similar for kriging and cokriging because the elevation data were located on a regular grid with a uniform spatial distribution throughout the UARW. The shape of the surface (not the magnitude) defined by kriging and cokriging estimation variances was determined primarily by the spatial distribution of the precipitation stations.

Estimation variances were reduced by 30% for cokriging relative to kriging over approximately 90% of the UARW (Fig. 5). The largest reduction of 65% resulted for a location south of Quartz Mountain, in the northwestern section of the UARW. Reductions of more than 60% were indicated for the Amargosa Desert in the south-central and western sections of the UARW, and reductions of 55% resulted at the potential repository site. In general, reductions in estimation variances of as much as 50% were indicated at distances of approximately 30,000 ft (6 mi) from precipitation stations. Reductions decreased for areas outside the boundaries of the UARW as a result of edge effects caused by the boundary of the elevation sample. Edge effects were most pronounced at the southern extent of the UARW, where the search neighborhood radius of 120,000 ft for elevation did not include any precipitation stations.

c. Validation of Cokriging and Kriging Estimates

The scatterplot of the kriging estimates indicated a lack of correlation with elevation in the range of -250 to 3,000 ft (Fig. 6). A correlation between kriging estimates and elevation was indicated for elevations above 3,000 ft, along with an increase in the variability of estimates. A regression equation was fit to the data:

$$AAP^{*} = \exp(4.51 + 0.000115), \quad r^2 = 0.46 \quad , \tag{4}$$

where AAP^{*} is the kriging estimate for AAP (mm) at a grid location and E is elevation

(ft) of the grid location. Equation 4 indicated a smaller orographic influence (i.e., the regression parameter multiplying E in Eq. 4 is smaller) for AAP than that defined by precipitation stations in the southern Nevada and southeastern California region (Equation 13, Hevesi et al., 19XX).

The scatterplot of the cokriging estimates indicated a stronger log-linear correlation between AAP and elevation than the correlation indicated by the kriged estimates (Fig. 7). A maximum cokriging estimate of 442 mm was obtained for the maximum elevation of 8,400 ft in the northern Spring Mountains, which was 155 mm greater than the maximum kriging estimate of 287 mm for an elevation of 7,500 ft, and 88 mm greater than the maximum measured value of AAP for an elevation of 6,100 ft in the Spring Mountains (station 215, Table 3, Hevesi et al., 19XX). A regression equation was fit to the cokriging estimates and elevations:

$$AAP^* = \exp(4.26 + 0.000197E), \quad r^2 = 0.79 \quad . \tag{5}$$

For the range of elevations representative of Yucca Mountain (3,000 to 6,000 ft), Eq. 5 defines a gradient of +31 mm AAP/1000 ft., which was the same as the observed gradient defined by the 42 precipitation stations used to develop the multivariate model (Hevesi et al., 19XX). Using Eq. 5, cokriging estimates of AAP are predicted to vary 28 mm within the area of the potential repository site, because the range of elevations overlying the area of the site is approximately 900 ft.

A comparison of the regression equations defined by Eqs. 4 and 5 with regression

equations presented in Hevesi et al. (19XX) using measured values of AAP indicated that the cokriged estimates preserved the expected relation between AAP and elevation, while the kriged estimates did not. This provided good evidence of model validation, indicating that the cross-variogram model, which was difficult to define (Hevesi et al, 19XX), represented a reasonable correlation between AAP and elevation.

The relation defined by Houghton et al (1975) between climate, elevation, and vegetation indicated a stronger orographic influence on AAP in the Great Basin than the correlation indicated by the regression curve obtained using cokriging estimates and curves obtained using measured values of AAP. The stronger correlation is partly due to lower average air temperatures in the northern Great Basin (which includes northern and central Nevada) relative to the southern Nevada and southeastern California regions. However, the lower limit for the "Moist Steppe" climatic zone (pinyon - juniper woodland), corresponding to an AAP value of 250 mm and an elevation of 5,900 ft, and the lower limit of the "Dry Steppe" climatic zone, corresponding to an AAP value of 200 mm and an elevation of 4,600 ft, indicated a relatively close fit to the regression equation defined by French (1986) for the 12 NTS stations, and a reasonable fit to the regression equation defined by the cokriging estimates.

d. Validation of Cokriging and Kriging Isohyetal Mappings

The location of the cokriging 250-mm AAP isohyet coincided closely with the location of pinyon pine and juniper woodland boundaries for most areas, whereas the

location of the kriging 250 mm isohyet did not (Fig. 8). A close match of the cokriging results with the woodland boundary was obtained for Pahute Mesa, Shoshone Mountain. Timber Mountain, Yucca Mountain. the Grapevine Mountains, and the Spring Mountains, and this indicated good estimation accuracy for these locations. The abscence of the kriging 250-mm isohyet in the Grapevine and Spring Mountains indicated that the expected orographic influence for these remote, mountainous locations was not adequately represented by the available sample of AAP measurements.

The 250-mm cokriging isohyet did not coincide with woodland boundaries at all locations. Cokriging estimates exceeding 250 mm occured at elevations above 6,000 ft in the Black Mountains (outside of the UARW) where pinyon pine and juniper woodlands were not observed. The cokriging estimates at these locations may have been erroneously high because of a rain-shadow effect from Telescope Peak and because there were no precipitation stations within the elevation search radius for grid locations in this area. The 250-mm cokriging isohyet did not coincide with the woodland boundary observed on the summit of Quartz Mountain, along the northwest edge of the UARW. Although the cokriging estimate of 180 mm was 40 mm greater than the kriging estimate for Quartz Mountain, a relatively low estimate of AAP was calculated for this location because the measured value of 90 mm AAP at the nearest precipitation station (station 228, Hevesi et al. 19XX), located within the deficit zone defined by French (1983), was also relatively low for the station elevation of 4,020 ft.

e. Usefulness of 1990 Active Stations for Isohyetal Mapping

Cokriging variances calculated for the active network of precipitation stations indicated significant improvements in the potential accuracy of estimating AAP at Yucca Mountain and in the vicinity of the potential repository site, but many locations within the UARW indicated an increase in cokriging variances relative to the historical network because several precipitation stations were no longer active at the time of this study (Fig. 9). A maximum estimation variance of 2,600 mm^2 within the UARW occurred at the southern extent of the watershed boundary, indicating an 18% increase relative to estimation variances obtained using the historical precipitation station network. High estimation variances exceeding 1,600 mm^2 within the UARW were also obtained along the western and northwestern edges of the watershed boundary, resulting in as much as a 33% increase in estimation variances relative to the historical network. In general, estimation variances were less than 1,000 mm^2 for 50% of the UARW, with minimum values located at Yucca Mountain and along the northeastern section of the watershed boundary. Cokriging estimation variances in the vicinity of the potential repository site were less than 400 mm^2.

f. Usefulness of Additional Fictitious Stations

Twenty locations for additional precipitation stations were identified within the UARW using maximum cokriging variances; the locations were numbered to indicate the sequence in which each separate location was added to the total network (Fig. 10). The 1st and 2nd identified locations occured within the Amargosa Desert in the southern

extent of the UARW, indicating this to be the most important area for locating additional precipitation stations. The Funeral Mountains, the Grapevine Mountains, Sarcobatus Flat, Quartz Mountain, and the northern extent of the Spring Mountains were also indicated as important locations for additional precipitation stations. Estimation variances obtained using the expanded network of 58 stations indicated large potential reductions in estimation variances for the northwestern, western, and southwestern sections of the UARW. In general, estimation variances were more uniform throughout the UARW relative to estimation variances obtained using the 1990 active network; variances within the UARW were less than 700 mm^2 at all locations, and were less than 500 mm^2 for approximately 40% of the UARW. Maximum reductions were obtained along the southern and western sections of the watershed boundary; 12 of the 20 identified locations were on the boundary. No reduction in estimation variances occurred in the vicinity of the potential repository site and throughout the entire northeast portion of the UARW because of the relatively dense cluster of active stations within the NTS and on Yucca Mountain.

The configuration of the 20 additional locations was not considered to be optimum because the locations were not identified simultaneously. For the procedure used in this study, each additional location remained fixed after it was identified, and this affected all successive locations. A procedure to simultaneously identify 20 locations from 747 potential locations was difficult because the computational time required for the large number of possible combinations was prohibitive. Alternatively, identifying locations for additional stations based on a procedure to minimize the average

estimation variance within the UARW may have been more appropriate for defining optimum locations. If the average estimation variance had been minimized, identified locations would have occured further inside the watershed, not on the watershed boundary, because the area of influence for each additional station would be considered. The resulting configuration probably would have been more efficient because a smaller number of additional stations would provide the same level of estimation accuracy. Unfortunately, the procedure to minimize the average estimation variance also required a prohibitively long computation time. A continuing effort is being made to develop a more efficient procedure to simultaneously identify optimum locations for as many as 20 additional stations using the average cokriging variance.

A plot of the observed maximum and average cokriging variance was used to investigate the relative importance of each successive fictitious station in reducing estimation variances (Figure 11). As expected, the maximum variance decreases much more rapidly than the average variance, and the addition of the first 3 to 4 stations provides the largest reductions. Using the additional 20 fictitious stations, the average estimation variance within the UARW was reduced by 52% from 974 mm^2 to 464 mm^2, and the maximum estimation variance was reduced by 78% from 2,690 mm^2 to 597 mm^2.

4. Summary and Conclusions

Kriging and cokriging were used to estimate average annual precipitation (AAP) at Yucca Mountain, the potential site for a high-level nuclear-waste repository, and a surrounding 2,600 mi^2 watershed, refered to as the Upper Amargosa River Watershed (UARW). The cokriging estimation procedure used the observed positive correlation between AAP and elevation, precipitation data for 42 stations in the southern Nevada and southeastern California region surrounding the site, and elevation data for 64 stations and 1,531 grid locations within and adjacent to the UARW. Isohyets defined using cokriging estimates conformed closely to elevation contours and displayed the expected orographic effect of mountainous terrain within the UARW. Cokriging estimates obtained within the UARW included a maximum estimate of 335 mm for an elevation of 7,400 ft on Pahute Mesa, a minimum estimate of 79 mm for an elevation of 2,200 ft in the Amargosa Desert, and an average estimate of 157 mm for the area of the UARW. The cokriging average estimate was 12 mm greater than the kriging average estimate because increased AAP for higher elevations in the Grapevine Mountains, the Funeral Mountains, and the Spring Mountains was not adequately represented by the available sample of AAP measurements. The average cokriging estimate of 172 mm AAP at 8 precipitation stations located in the vicinity of the potential repository site was 29 mm greater than the average kriging estimate, and the maximum cokriging estimate of 247 mm was 87 mm greater than the maximum kriging estimate for the 8 precipitation stations.

Cokriging estimation variances for the UARW were reduced by an average of 54% relative to kriging estimation variances, indicating a significant improvement in estimation accuracy obtained by using elevation data. Cokriging estimation variances were reduced by 55% relative to kriging variances at the potential repository site, with maximum reductions of more than 60% occuring for large areas to the northwest and southwest of the site. Reductions of 50% were obtained at distances of approximately 30,000 ft (6 mi) from measured values of AAP.

Regression results between cokriging estimates of AAP and elevation compared favorably with regression results obtained between measured AAP and elevation, indicating that the correlation between AAP and elevation defined by the multivariate geostatistical model was reasonable. An indirect confirmation of the cokriging estimates was obtained by comparing the location of the estimated 250-mm isohyet relative to boundaries defining the occurrence of pinyon pine and juniper woodlands which were considered to be representative of the approximate lower limit of the moist steppe climatic zone in the southern Great Basin. In most cases, the location of the cokriging 250-mm isohyet corresponded closely with the woodland boundaries

The potential accuracy of the 1990 network of 38 active precipitation stations for estimating AAP was evaluated using cokriging estimation variances, and locations for 20 additional stations were selected using maximum cokriging estimation variances. Analysis of the expanded, hypothetical network indicated that precipitation stations were needed at low elevations in the Amargosa Desert throughout the southern section of the UARW, in Sarcobatus Flat in the northwest section of the UARW, and at the higher

elevations of Quartz Mountain, the Grapevine Mountains, the Funeral Mountains, and the northern Spring Mountains. These locations would be useful for improving precipitation characterization within the UARW based on both the elevation - precipitation correlation and the spatial distribution of precipitation measurements.

Acknowledgments. This work was done in cooperation with the U.S. Department of Energy, interagency agreement DE-AI08-78ET44802.

References

Cooper, R. M. and J. D. Istok. 1988: Geostatistics applied to groundwater contamination. I: Methodology - *J. Environ. Engrg.*, 114, 270-286.

Czarnecki, J. B., 1985: Simulated effects of increased recharge on the ground-water flow system of Yucca Mountain and vicinity, Nevada-California. U.S. Geological Survey Water-Resources Investigation Report 84-4344, 38 p.

Dingman, S. L., D. M. Seely-Reynolds, and R. C. Reynolds III, 1988: Application of kriging to estimating mean annual precipitation in a region of orographic influence. *Wat. Res. Bull.*, 24, 329-339.

French, R. H., 1983: A Preliminary Analysis of Precipitation in Southern Nevada. Water Resources Center, Desert Research Institute, Las Vegas, Nevada, DOE/NV/10162-10, 39 p.

French, R. H., 1986: Daily, Seasonal, and Annual Precipitation at the Nevada Test Site, Nevada. U.S. Dept. of Energy, Nevada Operations Office, No. DE-AC08-85NV10384, Publication No. 45042, 40 p.

Hevesi, J. A., J. D. Istok, and A. L. Flint, 1991: Precipitation estimation in mountainous terrain using multivariate geostatistics: 1. structural analysis. submitted to *Journal of Applied Meteorology.*

Houghton, J. G., C. M. Sakamoto, and R. O. Gifford, 1975: Nevada's weather and climate. University of Nevada, Reno, Mackay School of Mines, Bureau of Mines and Geology Special Publication No. 2.

Istok, J. D. and R. M. Cooper, 1988: Geostatistics applied to groundwater contamination. III. global estimates. *J. Environ. Engrg.*, 114, 915-928.

Journel, A.G. and C.J. Huijbregts, 1978: Mining Geostatistics. Academic Press, New York, N.Y. 600 p.

a.k.a. McMahon, 1985 – cited on p.3

Montazer, P. and W. E. Wilson, 1984: Conceptual hydrologic model of flow in the unsaturated zone, Yucca Mountain, Nevada. U.S. Geological Survey Water-Resources Investigations Report 84-4345, 55 p.

Quiring, R. F., 1983: Precipitation Climatology of the Nevada Test Site. Nuclear Support Office, Las Vegas, N.V.

Winograd, I. J. and W. Thordarson, 1975: Hydrogeologic and hydrochemical framework, south-central Great Basin, Nevada-California, with special reference to the Nevada Test Site. U.S. Geological Survey Professional Paper 712-C, 126 p.

AUTHORS: CROSS CHECK THIS TABLE AGAINST TABLE 3 IN COMPANION REPORT. SOME NAMES/NUMBERS DIFFER.

Table 1. Active Precipitation Stations in Southern Nevada and Southeastern California

Station Name	Nevada Central State Plane Coordinates Easting Coord. (ft)	Northing Coord. (ft)	Station Elevation (ft)	Years of Record	Measured Average Annual Precipitation (mm)	
Regional Stations						
Boulder City	1,029,489	490,470	2,525	50	139	
Caliente	1,133,802	995,954	4,407	51	231	
Las Vegas Airport	936,479	519,841	2,162	33	104	
Pioche	1,119,116	1,084,068	6,120	44	313	
Red Rock Summit	828,783	534,527	6,500	8	270	
Searchlight	1,009,908	338,717	3,540	50	185	
Beatty	472,943	785,458	3,550	47	159	*
Death Valley	437,164	627,537	-168	18	69	
Desert Game Rng.	887,736	622,641	2,920	42	106	
Dyer	100,904	991,059	4,975	31	125	
Goldfield	330,981	1,015,535	5,690	39	136	
Mina	76,428	1,216,240	4,551	53	115	
Pahrump	691,717	559,004	2,700	20	125	
Rattlesnake	644,277	1,235,821	5,912	20	163	
Nevada Test Site Stations						
Rock Valley	639,050	704,700	3,400	8	157	*
Desert Rock A.P.	688,100	681,750	3,298	15	157	*
Mercury	696,738	695,045	3,770	13	159	*
4JA	610,605	740,840	3,422	16	119	*
Cane Springs	663,600	751,000	4,000	21	208	
Well 5B	705,200	747,600	3,080	19	128	
Mid Valley	644,500	809,250	4,660	13	226	
Yucca	680,875	837,100	3,920	25	176	
40 MN	610,600	837,100	4,820	18	202	*
Tippipah Spring	638,650	838,600	4,980	20	245	
BJY	679,100	842,300	4,072	22	176	
Area 12 Mesa	631,400	888,900	7,490	17	295	*
PHS Farm	682,870	895,840	4,565	8	192	
Little Feller 2	602,000	858,520	5,160	8	229	
Pahute Mesa #1	566,700	909,700	6,550	4	212	*
Jackass Flat	610,564	743,968	3,492	0		*

Table 1. Continued

Station Name	Nevada Central State Plane Coordinates Easting Coord. (ft)	Northing Coord. (ft)	Station Elevation (ft)	Years of Record	Measured Average Annual Precipitation (mm)	
Yucca Mountain Stations						
UZ-1	560,148	771,482	4,432	4	203	*
UZ-6	558,356	760,134	4,915	2	176	*
SAIC-60	569,155	761,832	3,750	0		*
Prow	554,986	782,850	5,870	0		*
RF-1	567,934	759,011	3,815	0		*
Fran Ridge	573,575	754,015	4,062	0		*
USW G-3	560,265	751,136	4,765	0		*
Alice Point	577,000	770,000	4,047	0		*

* Precipitation Stations located within Upper Amargosa River Watershed (UARW) Boundary

Table 2. Summary of Results for Estimated AAP Within the UARW.

Statistic for UARW	Measured AAP from 10 Stations Within UARW (mm)	Estimates of AAP for 747 Grid Locations Within UARW: Cokriging Estimates (mm)	Kriging Estimates (mm)	Cokriging Estimation Variances (mm^2)	Kriging Estimation Variances (mm^2)
Average	179	157	145	836	1,808
Maximum	295	335	287	2,490	3,460
Minimum	85	79	86	290	256
Variance	3,280	2,488	1,519	87,280	582,058

Range of Estimated AAP Within UARW (mm)	Percent Area of UARW Within Range of Estimated AAP: Cokriging (%)	Kriging (%)
> 300	0.9	0.0
300 - 250	4.3	1.9
250 - 200	14.1	8.8
200 - 150	29.0	30.9
150 - 100	42.4	49.4
< 100	9.2	11.4

Table 3 **Estimates of AAP at 10 Precipitation Stations Within the UARW. Location Coordinates for the Stations are Listed in Table 1.**

Precipitation Station Name	Station Elevation (ft)	Cokriged AAP (mm)	Kriged AAP (mm)	Cokriged Estimation Variance (mm^2)	Kriged Estimation Variance (mm^2)
Pahute Mesa #1	6,550	270	214	1,060	2,250
Jackass Flat	3,492	131	133	375	441
Prow	5,870	247	160	764	1,790 *
UZ-6	4,915	184	139	752	1,710 *
USW G-3	4,765	165	130	783	1,650 *
UZ-1	4,432	171	150	757	1,720 *
Fran Ridge	4,062	151	135	698	1,450 *
Alice Point	4,047	158	151	698	1,470 *
RF-1	3,815	149	138	723	1,580 *
SAIC-60	3,750	145	141	721	1,570 *
Average for 8 stations located on Yucca Mountain	4,457	172	143	737	1,617

* Precipitation stations located on Yucca Mountain, in the vicinity of the potential repository site.

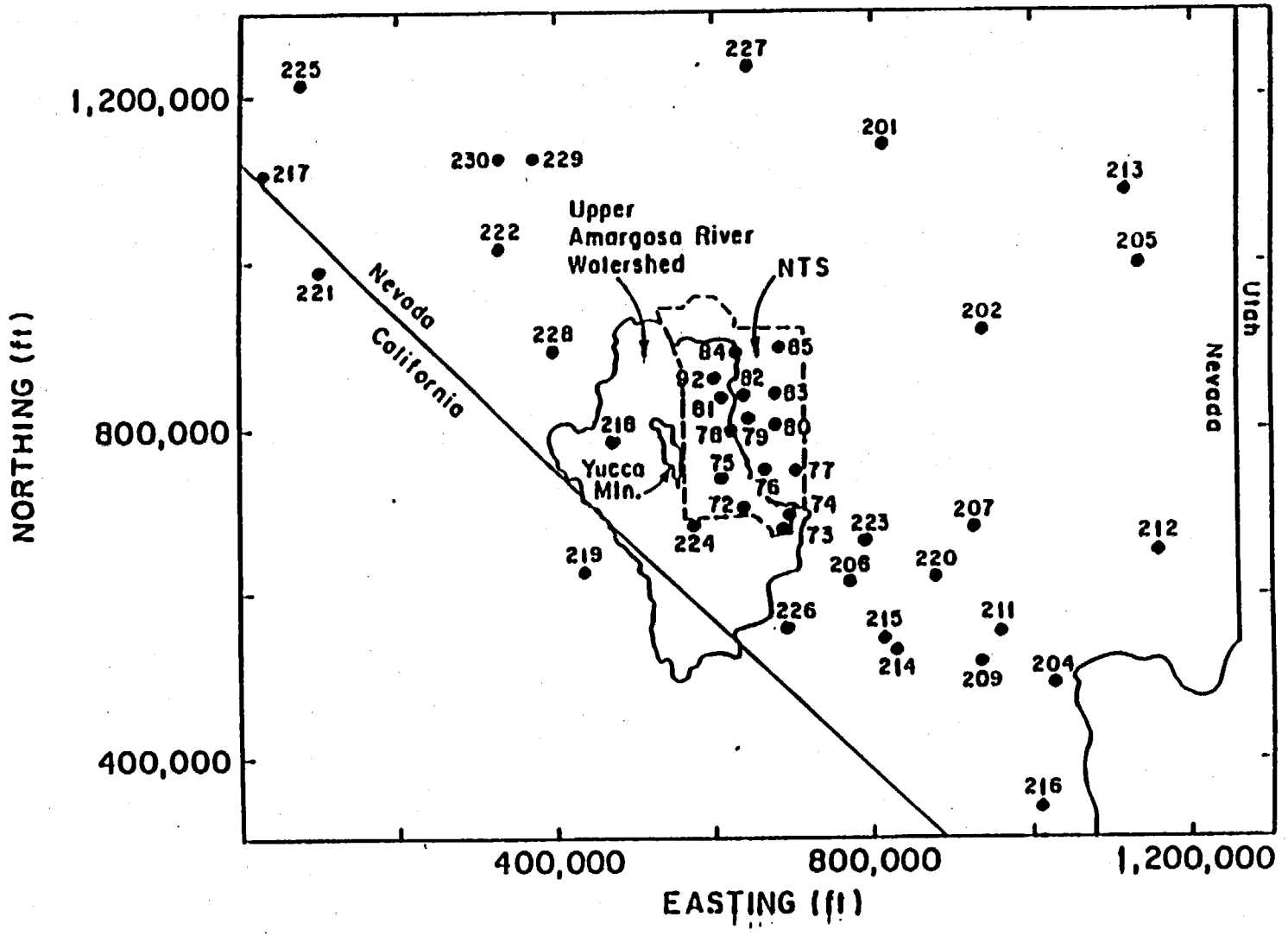
NORTHING (ft)
1,200,000
800,000
400,000
400,000
800,000
1,200,000
EASTING (ft)
Upper
Amargosa River
Watershed
NTS
Nevada
California
Utah
Nevada
Yucca
Mtn.
225
227
201
230
229
213
217
222
205
221
202
228
84
85
92
82
83
81
218
78
79
80
75
77
76
72
74
224
73
223
207
212
219
206
220
226
215
211
214
209
204
216

FIGURE 1

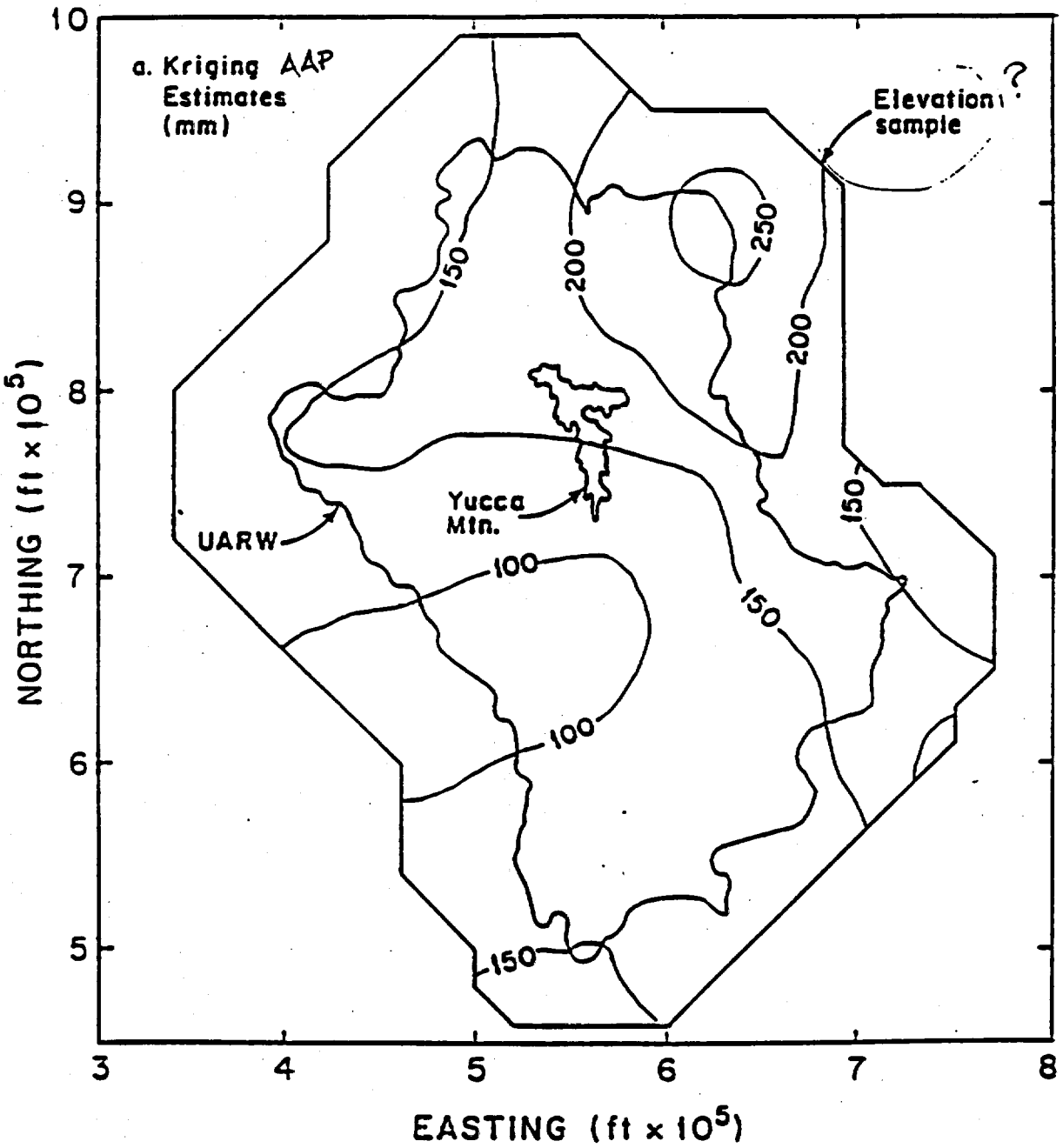
a. Kriging AAP Estimates (mm)
Elevation sample
Yucca Mtn.
UARW
150
200
250
200
150
100
150
100
150
NORTHING (ft x 10^5)
EASTING (ft x 10^5)
10
9
8
7
6
5
3
4
5
6
7
8

FIGURE 2a

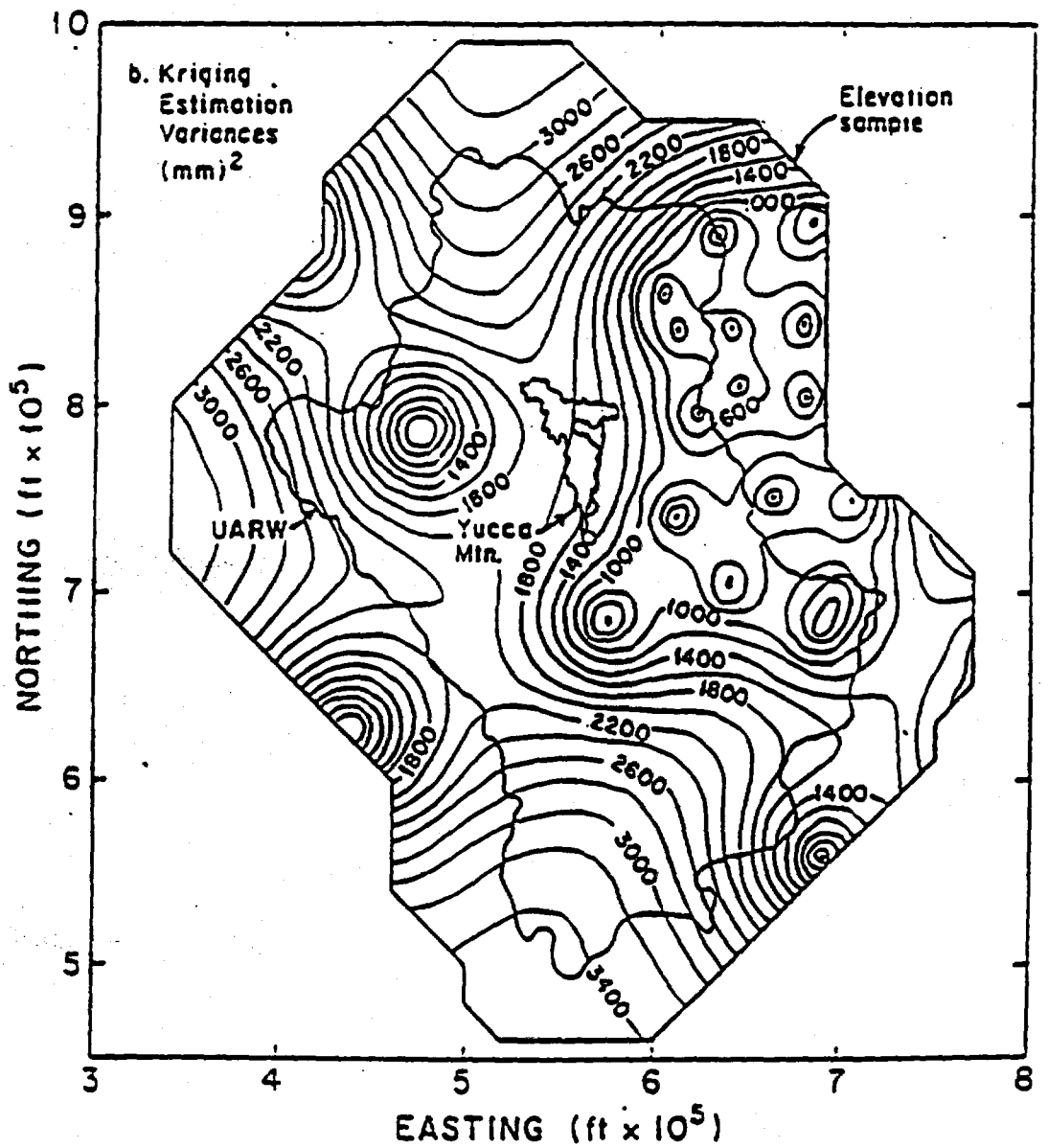
b. Kriging Estimation Variances (mm)²
Elevation sample
UARW
Yucca Mtn.
NORTHING (ft x 10⁵)
EASTING (ft x 10⁵)
10
9
8
7
6
5
3
4
5
6
7
8
3000
2600
2200
1800
1400
1000
600
3400

FIGURE 2b

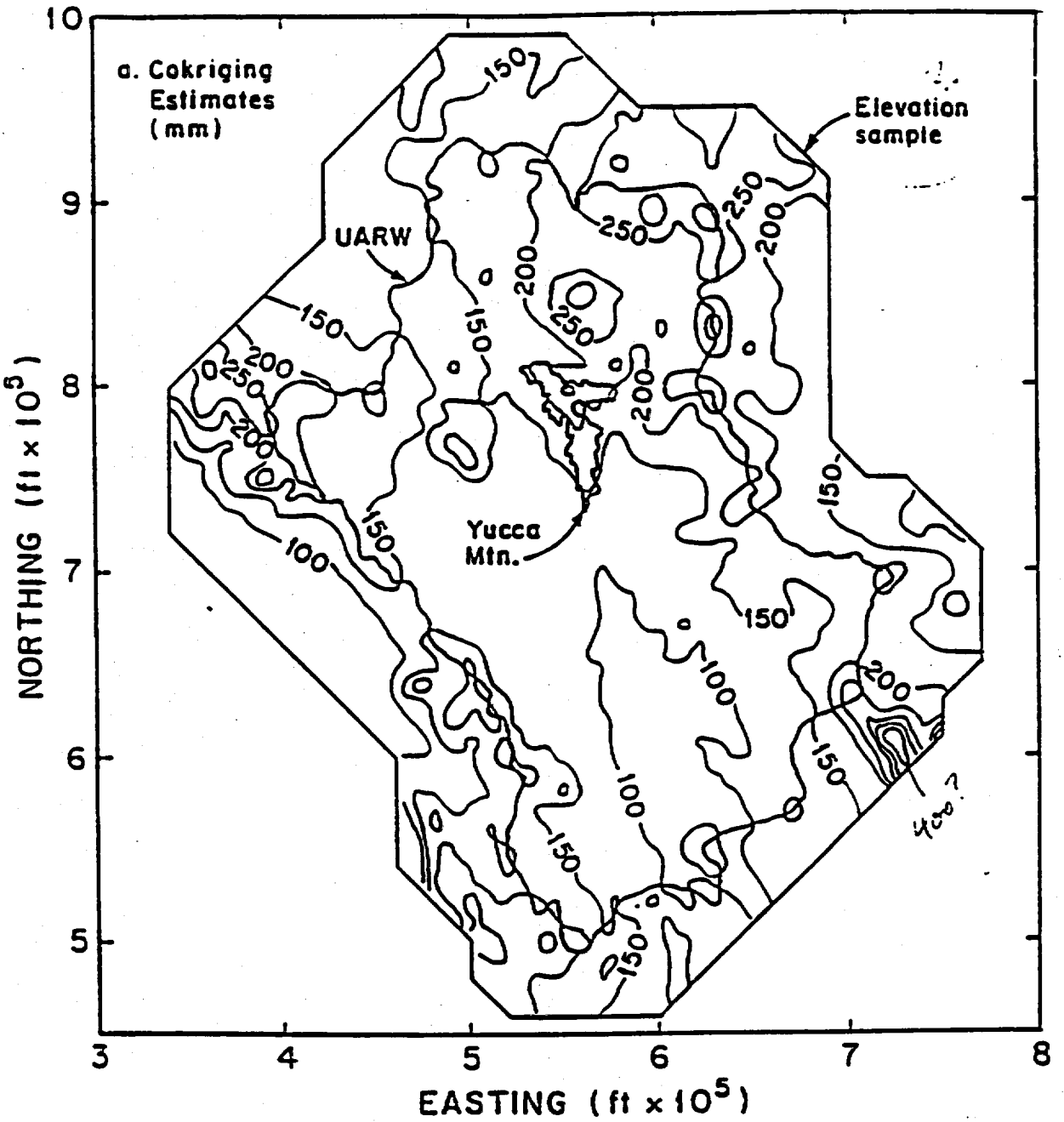
a. Cokriging Estimates (mm)
Elevation sample
UARW
Yucca Mtn.
NORTHING (ft x 10^5)
EASTING (ft x 10^5)
10
9
8
7
6
5
3
4
5
6
7
8
0
100
150
200
250
400?

FIGURE 3a

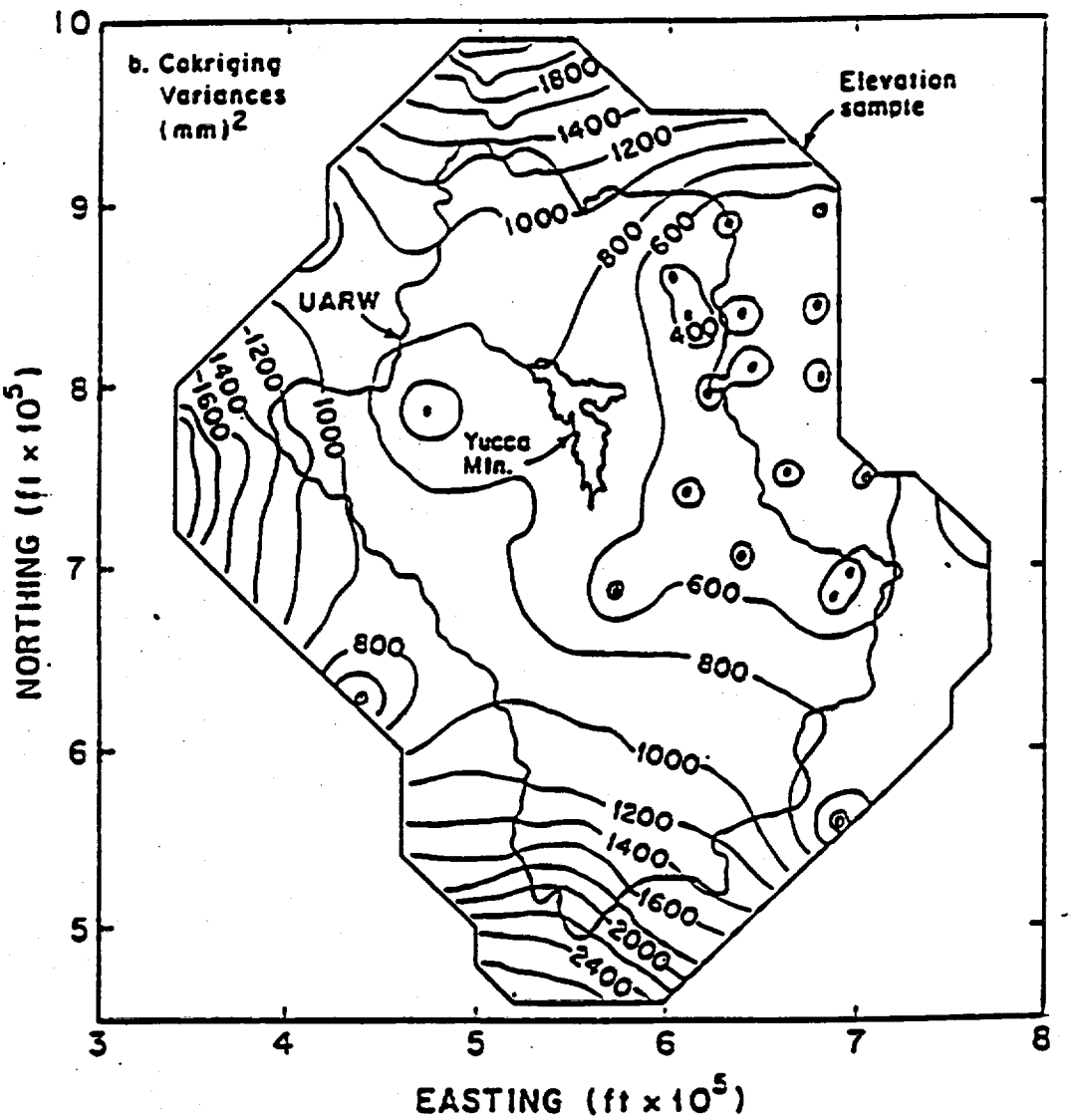
b. Cokriging Variances (mm)2
Elevation sample
UARW
Yucca Mtn.
1800
1400
1200
1000
800
600
400
1200
1400
1600
1000
800
600
800
1000
1200
1400
1600
2000
2400
NORTHING (ft x 10^5)
EASTING (ft x 10^5)
10
9
8
7
6
5
3
4
5
6
7
8

FIGURE 3b

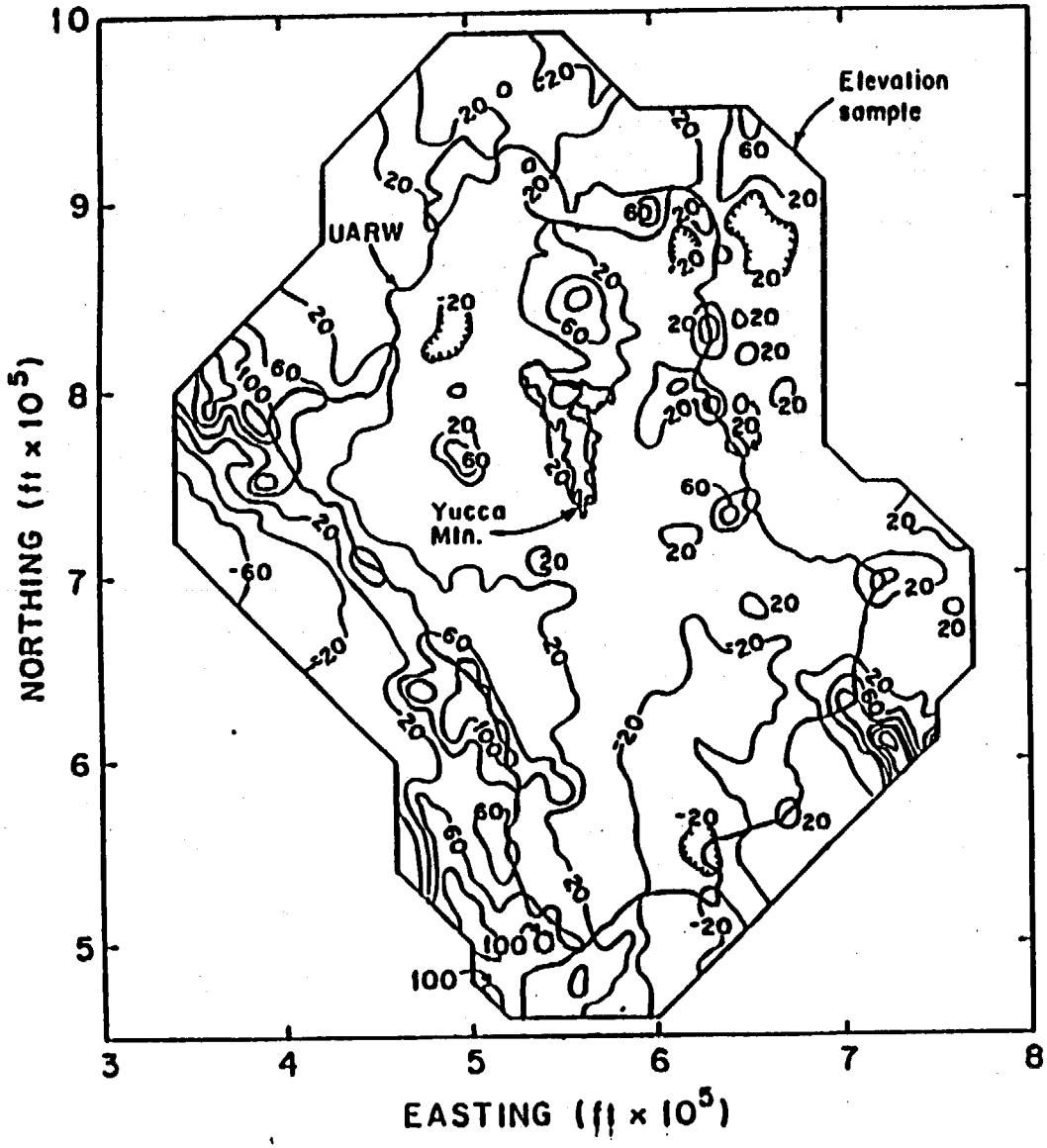
Elevation sample
UARW
Yucca Min.
NORTHING (ft x 10^5)
EASTING (ft x 10^5)
10
9
8
7
6
5
3
4
5
6
7
8

FIGURE 4

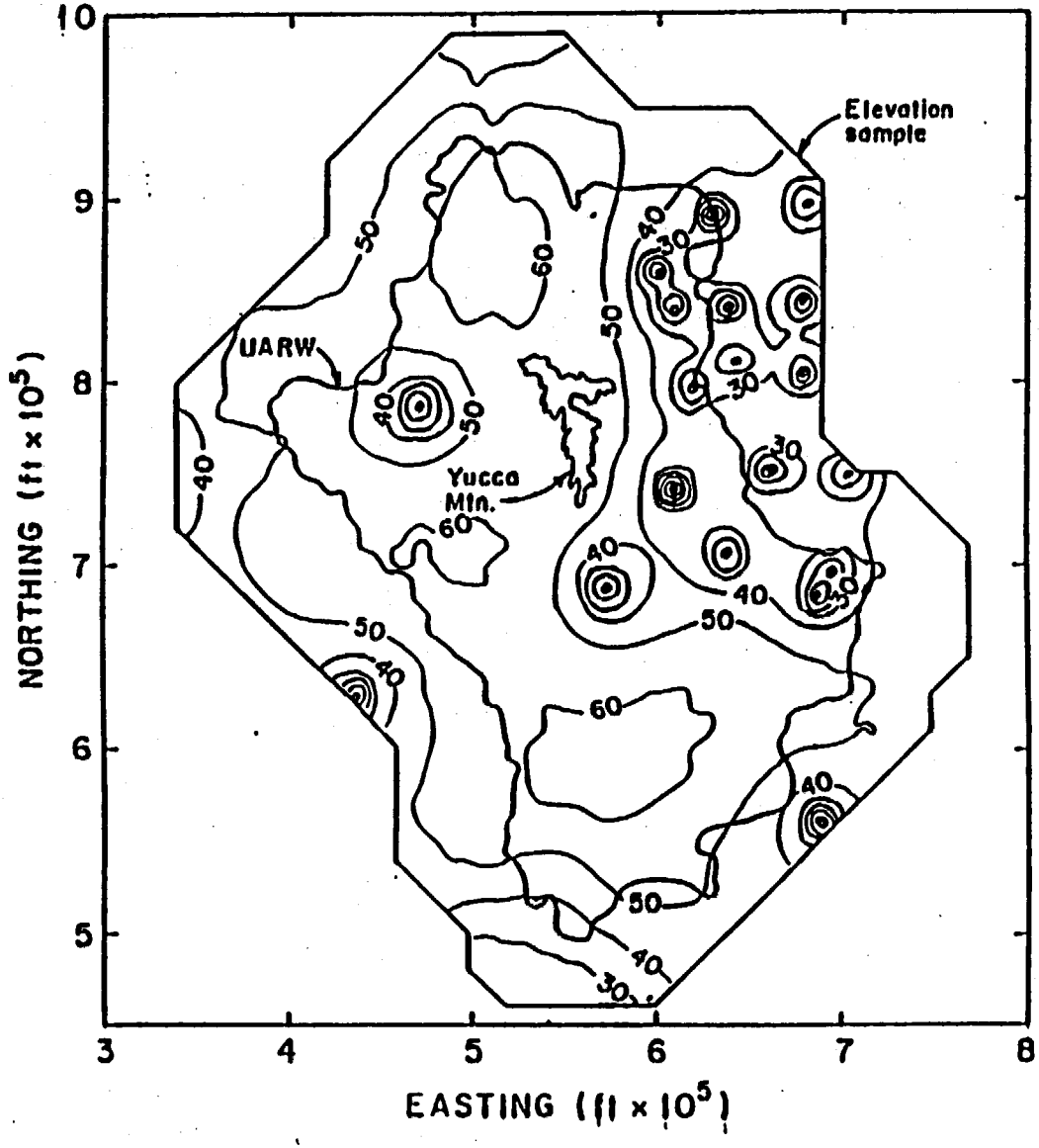
Elevation sample
UARW
Yucca Mtn.
NORTHING (ft x 10^5)
EASTING (ft x 10^5)
10
9
8
7
6
5
3
4
5
6
7
8
30
40
50
60

FIGURE 5

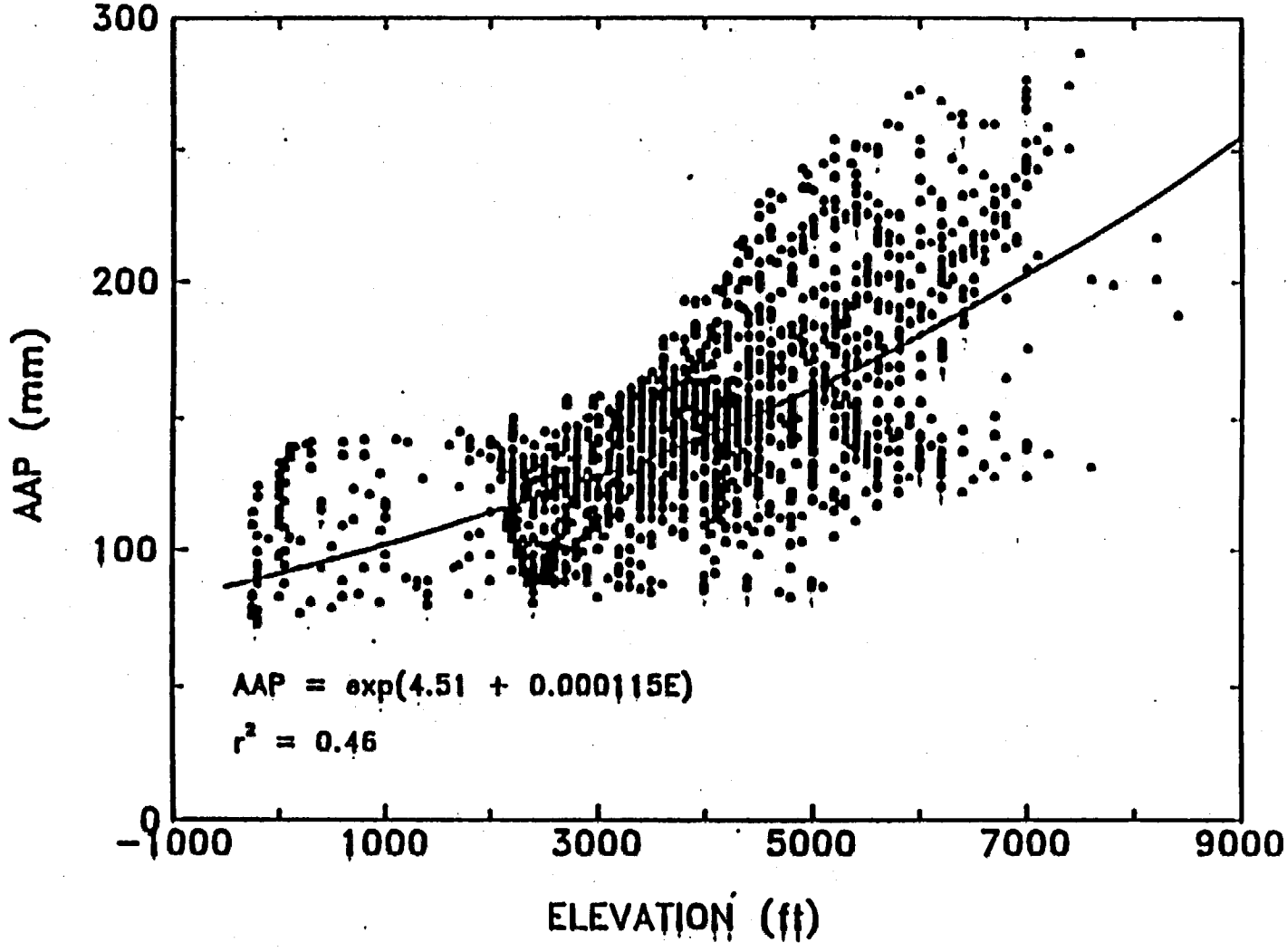
300
200
100
0
AAP (mm)
AAP = exp(4.51 + 0.000115E)
r² = 0.46
-1000
1000
3000
5000
7000
9000
ELEVATION (ft)

FIGURE 6

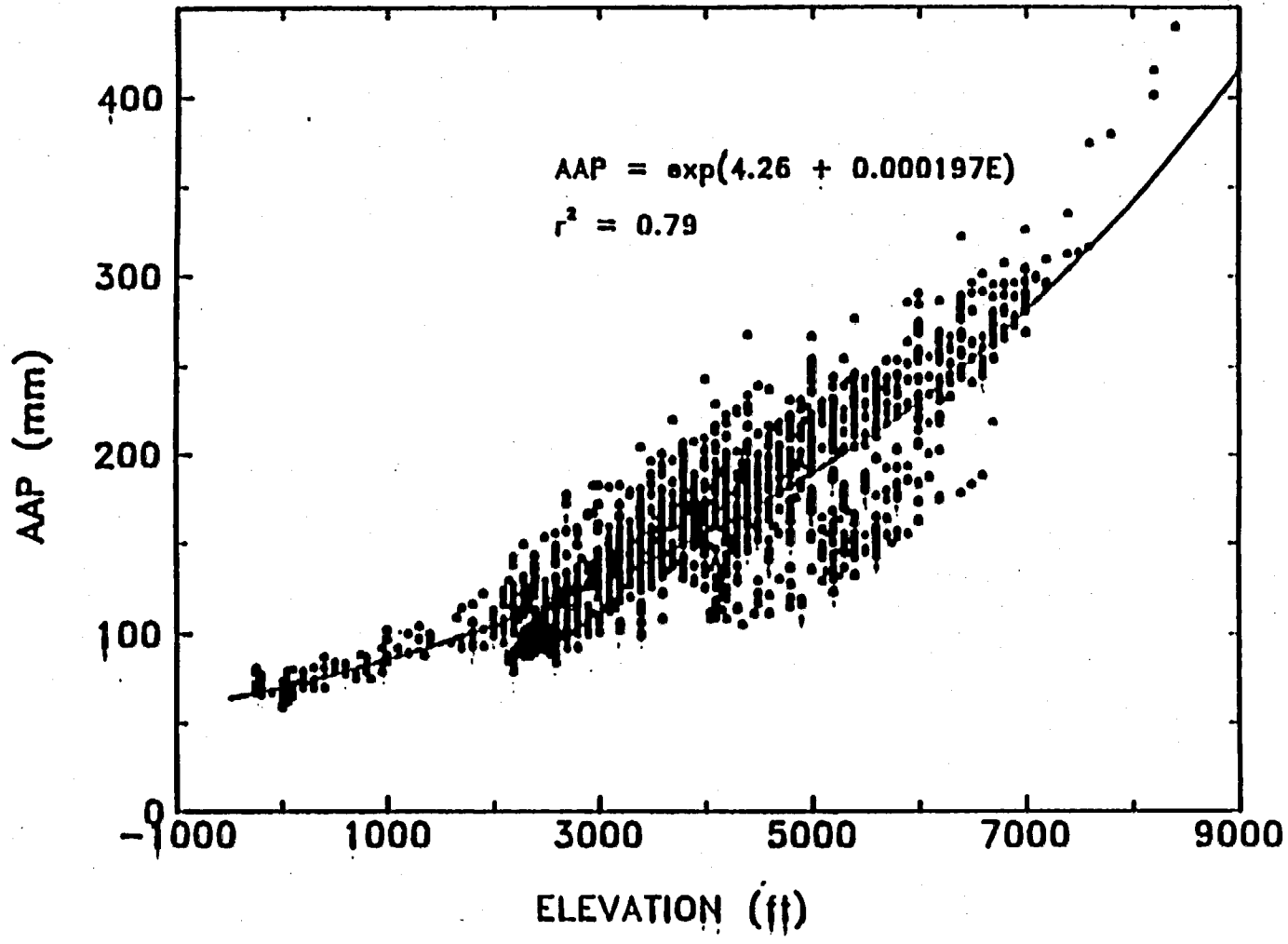
AAP = exp(4.26 + 0.000197E)
r² = 0.79
AAP (mm)
ELEVATION (ft)
0
100
200
300
400
-1000
1000
3000
5000
7000
9000

FIGURE 7

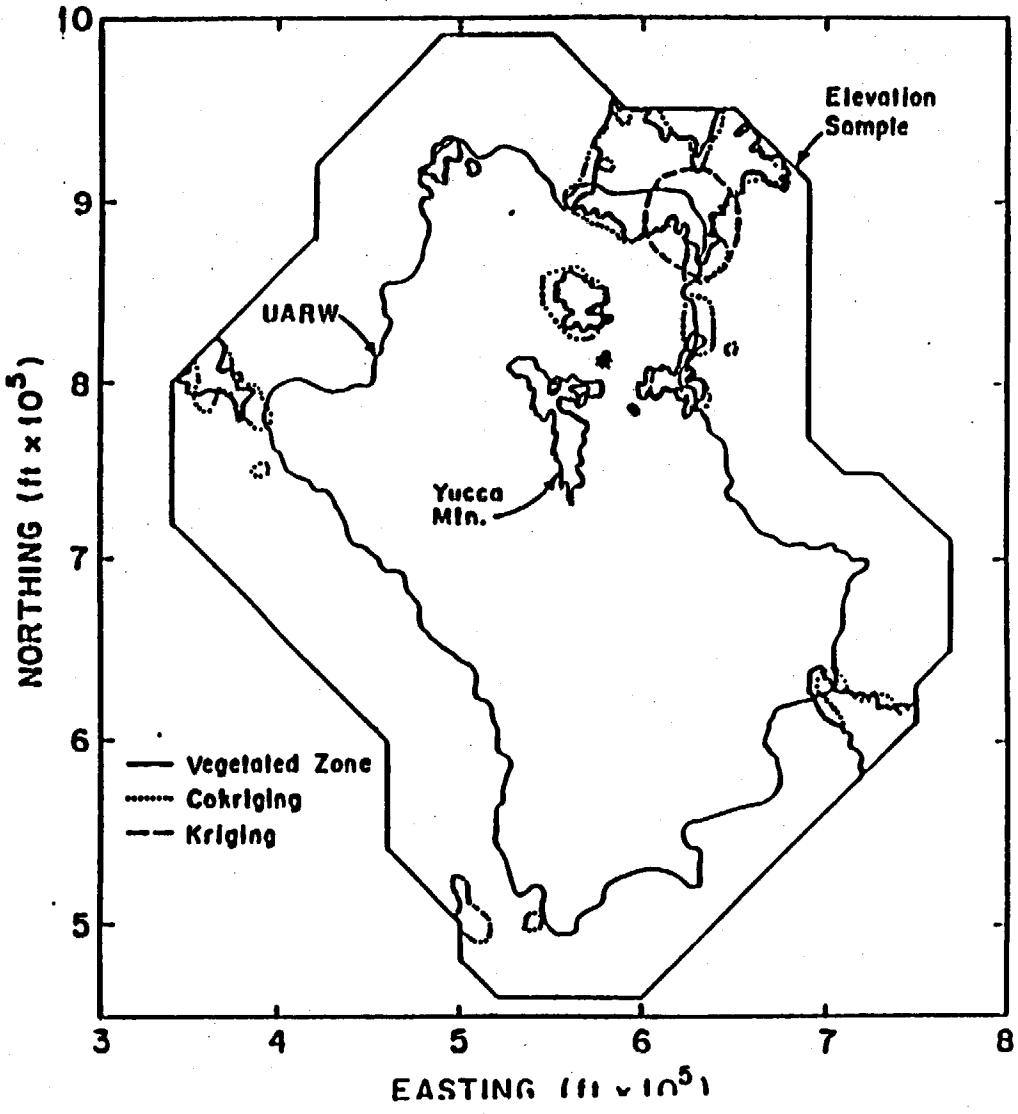
10
9
8
7
6
5
3
4
5
6
7
8
NORTHING (ft x 10^5)
EASTING (ft x 10^5)
Elevation Sample
UARW
Yucca Mtn.
Vegetated Zone
Cokriging
Kriging

FIGURE 8

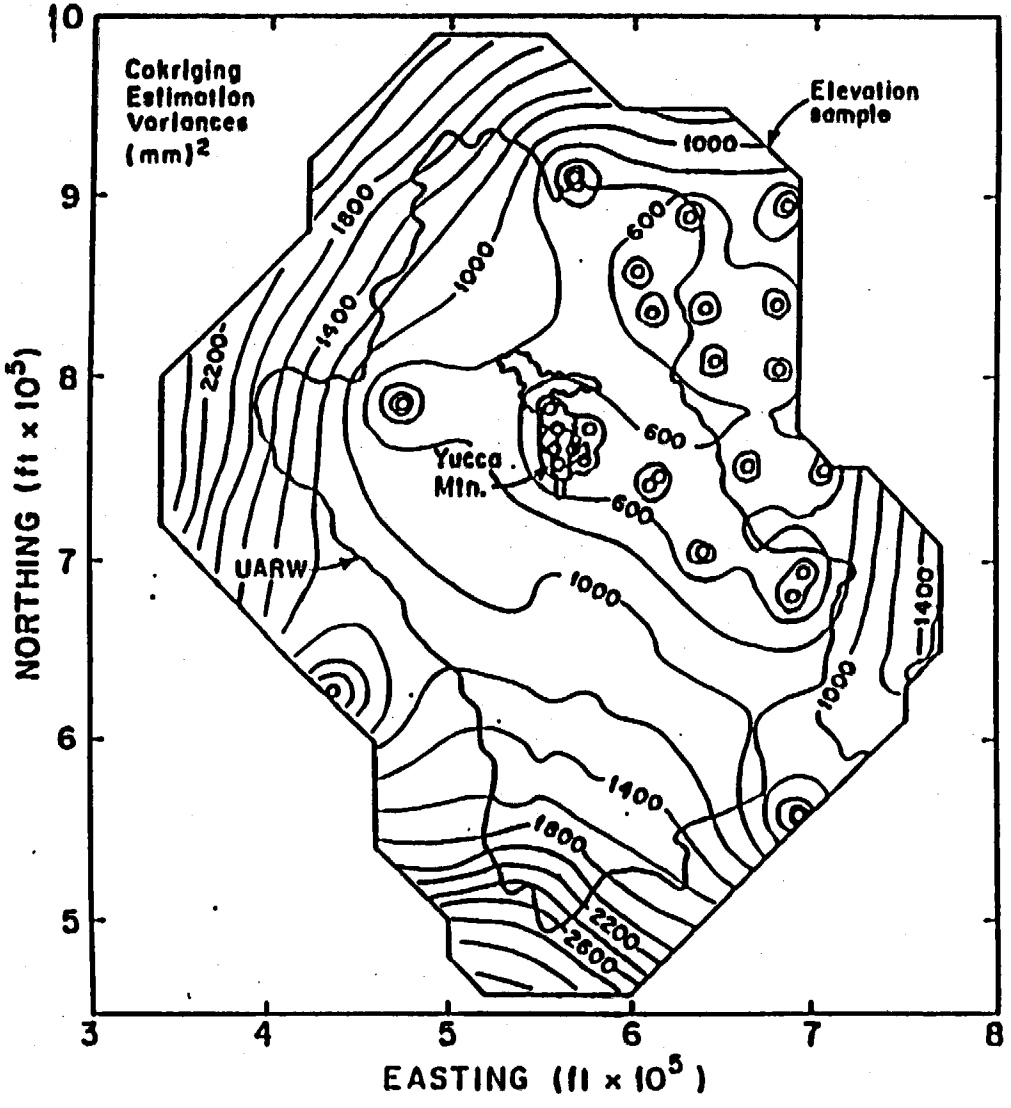
Cokriging
Estimation
Variances
(mm)²
Elevation
sample
1000
600
1800
1000
1400
2200
600
Yucca
Mtn.
600
UARW
1000
1400
1000
1400
1800
2200
2600
10
9
8
7
6
5
3
4
5
6
7
8
NORTHING (ft x 10⁵)
EASTING (ft x 10⁵)

FIGURE 9

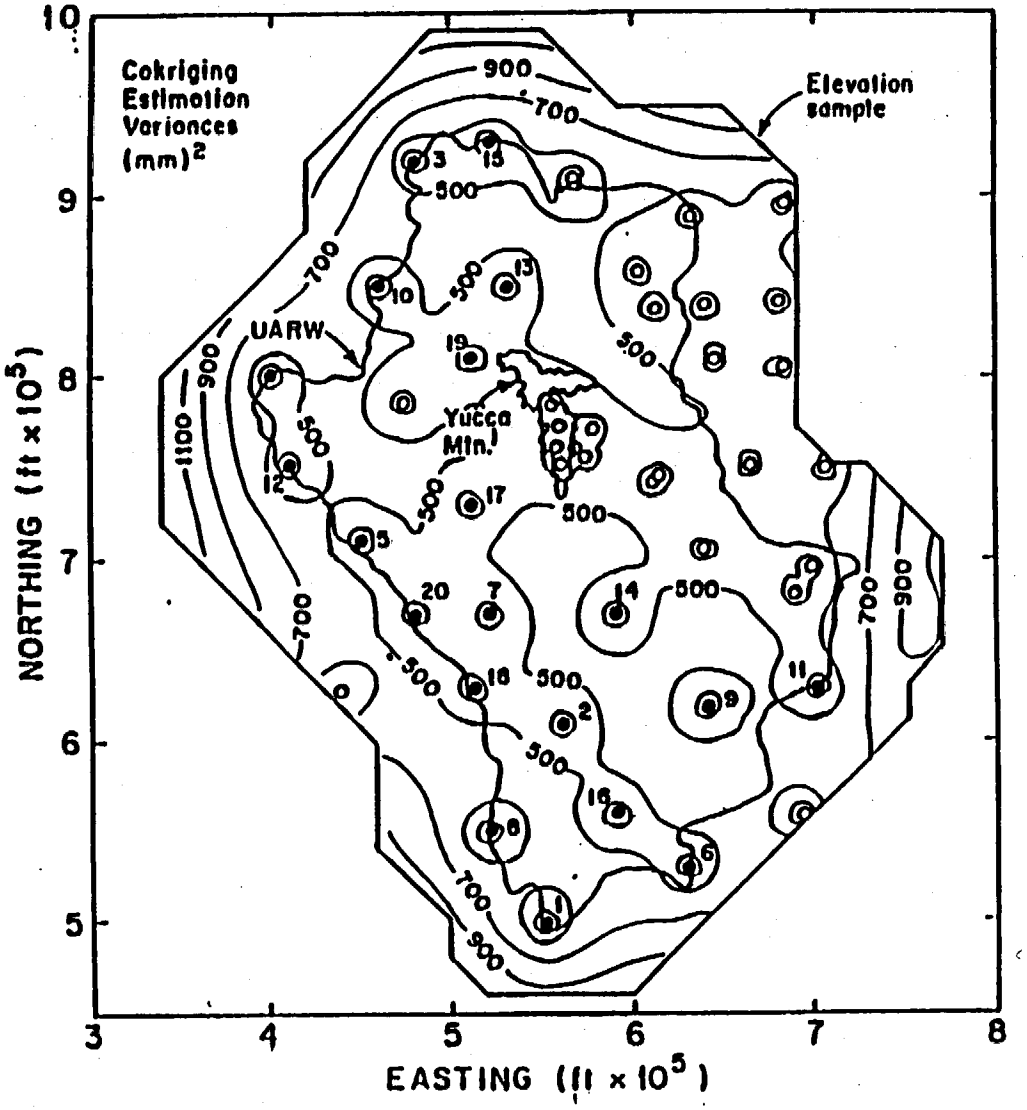
Cokriging
Estimation
Variances
(mm)²
Elevation
sample
UARW
Yucca
Mtn.
900
700
500
1100
NORTHING (ft × 10⁵)
EASTING (ft × 10⁵)
10
9
8
7
6
5
3
4
5
6
7
8

FIGURE 10

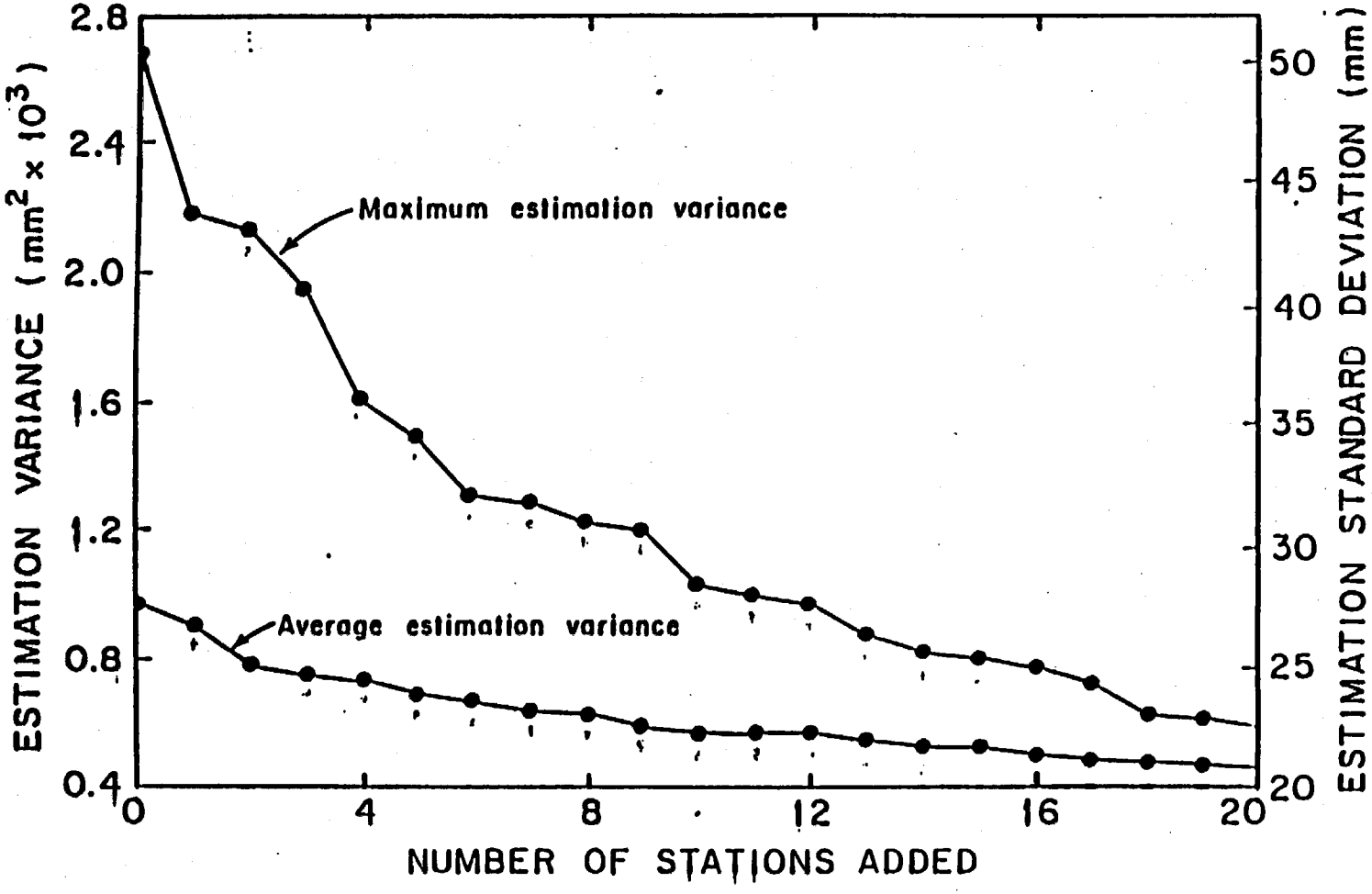
ESTIMATION VARIANCE (mm² x 10³)
2.8
2.4
2.0
1.6
1.2
0.8
0.4
Maximum estimation variance
Average estimation variance
0
4
8
12
16
20
NUMBER OF STATIONS ADDED
50
45
40
35
30
25
20
ESTIMATION STANDARD DEVIATION (mm)

FIGURE 11

PART 2, VOLUME I

The Joint NASA/Geosat Test Case Project

Final Report

Michael J. Abrams
James E. Conel
Harold R. Lang
Jet Propulsion Laboratory
California Institute of Technology
Pasadena, California

Editor
Helen N. Paley
Jet Propulsion Laboratory

October 1984

AAPG BOOKSTORE
P.O. Box 979
Tulsa, OK 74101, USA

Enclosure 3
8.3.1.2.2.1

The research described in this publication was carried out jointly by the Jet Propulsion Laboratory, California Institute of Technology, under a contract with the National Aeronautics and Space Administration, and by The Geosat Committee, Inc., and its members.

Published by
The American Association of Petroleum Geologists
Tulsa, Oklahoma 74101, USA

ISBN: 0-89181-654-2
Library of Congress Cataloging in Publication Data

Abrams, Michael J.
The Joint NASA/Geosat Test Case Project.

Sponsored by NASA, Jet Propulsion Laboratory, and Geosat
October 1984
Includes bibliographies
1. Joint NASA/Geosat Test Case Project. 2. Geology—Remote sensing. 3. Petroleum—Geology—Remote sensing. 4. Mines and mineral resources—Remote sensing. I. Conel, James E. II. Lang, Harold R. III. Paley, Helen N. IV. United States. National Aeronautics and Space Administration. V. Jet Propulsion Laboratory (U.S.) VI. Geosat Committee. VII. Title.
QE33.2.R4A27 1985 622'.1 85-1381